

An-Najah National University

Faculty of Graduate Studies

**Dual functionalization of single-walled carbon nanotubes for
targeted cancer therapy**

By

Safa' Raed Dayyeh

Supervisor

Dr. Mohyeddin Assali

Co-Supervisor

Dr. Naim Kittana

**This Thesis is Submitted in Partial Fulfillment of the Requirements for
the Degree of Master in Pharmaceutical Sciences, Faculty of Graduate
Studies, An-Najah National University, Nablus-Palestine.**

2018

**Dual functionalization of single-walled carbon nanotubes for
targeted cancer therapy**

By

Safa' Raed Dayyeh

This Thesis was defended successfully on 07/05/2018 and approved by:

Defense Committee Members

Signature

1. Dr. Mohyeddin Assali / Supervisor

.....

2. Dr. Naim Kittana /co-Supervisor

.....

3. Dr. Numan Malkieh / External Examiner

.....

4. Dr. Murad Abu Alhasan / Internal Examiner

.....

Dedication

To the most affectionate and greatest father and mother in the world who are supporting me, carrying my burdens, forgiving my mistakes and standing beside me until became what I am now.

To my Sister Nisreen and my brothers Mo'men and Mo'tasem.

To my lovely fiancé Bara' who supported me each step of the way and has been my constant source of inspiration.

To my friends and every person have given me the drive and discipline to tackle any task with enthusiasm and determination.

I dedicate this work

Acknowledgement

Firstly, I thank the holy god for giving me the strength, ability, qualifications and the patience to complete this research.

Then, I want to thank my thesis supervisors: Dr. Mohyeddin Assali for all his support and the valuable guidance and advice in all portion of my research, his willingness to motivate me contributed tremendously to my research. In addition, special thanks to Dr. Naim Kittana for his scientific support, guidance and constructive advice.

I would like to thank the rest of examination committee, for reading my thesis, their insightful comments and suggestions and invaluable criticisms.

Thanks to Hamdi Mango Center for Scientific Research, Faculty of Medicine and Faculty of Science at the University of Jordan for their collaboration in NMR, TEM and TGA measurements.

Special and deepest thanks to the staff of the laboratories of the College of Pharmacy, Science and Medicine for providing help and assistance, especially the supervisor of the laboratories of the College of Pharmacy Mr. Mohammad Arar and the lab workers Tahreer Shtayeh and Linda Arar.

My friends and colleagues in the Department of Pharmacy deserve warm thanks, for their assistance, support and the most beautiful fun time that we spend it together during the period of my study.

My family, which doesn't have any words to express my love, thanks and gratitude to them for their psychological and moral support throughout the years of my studies and work in my research. I hope you will be proud of me.

Safa' Dayyeh

الإقرار

أنا الموقعة أدناه موقعة الرسالة التي تحمل العنوان:

Dual functionalization of single-walled carbon nanotubes for targeted cancer therapy

أقر بأن ما اشتملت عليه الرسالة هو نتاج جهدي الخاص، باستثناء ما تمت الإشارة إليه حيثما ورد، وأن هذه الرسالة ككل، أو أي جزء منها لم يقدم من قبل لنيل أي درجة أو لقب علمي أو بحثي لدى أي مؤسسة تعليمية أو بحثية أخرى.

Declaration

The work provide in this thesis, unless otherwise referenced, is the researcher's own work, and has not been submitted elsewhere for any other degree or qualification.

Student's name:

اسم الطالب:

Signature:

التوقيع:

Date:

التاريخ:

Table of contents

No	Content	Page
	Dedication	iii
	Acknowledgement	iv
	Declaration	vi
	List of Tables	ix
	List of Figures	x
	List of Schemes	xi
	List of abbreviations	xii
	Abstract	xiv
	Chapter one: Introduction	1
1.1	Cancer	1
1.2	Carbon nanotubes (CNTs)	5
1.3	Functionalization of CNTs	6
1.3.1	Non-covalent functionalization	7
1.3.2	Covalent functionalization	8
1.4	Doxorubicin	10
1.5	Literature Review	12
1.6	Aims of the study	14
1.7	Objectives	14
1.8	General approach of the synthesis and functionalization of SWCNTs	15
	Chapter Two: Methodology	17
2.1	Reagents and materials	17
2.2	Instrumentation	18
2.3	Synthesis and characterization of the products	19
2.3.1	Synthesis of Tosyl-TEG-OH (1)	19
2.3.2	Synthesis of OH-TEG-N3 (2)	20
2.3.3	Synthesis of N3-TEG-nitrophenyl carbonate (3)	21
2.3.4	Synthesis of hydrazine derivative (4)	22
2.3.5	Synthesis of SWCNTs-alkyne (5)	22
2.3.6	Functionalization of f-SWCNTs 5 with compound 4 (6)	23
2.3.7	Functionalization of f-SWCNTs 6 with Doxorubicin (7)	24
2.3.8	Synthesis of 4-aminophenyl α -D-mannopyranoside (8)	24
2.3.9	Functionalization of SWCNTs-Alkyne with compound 8 (9)	25
2.3.10	Functionalization of f-SWCNTs 9 with compound 4 (10)	26
2.3.11	Functionalization of f-SWCNTs 10 with Doxorubicin (11)	27
2.4	In vitro drug release	27

2.4.1	Calibration curve of Doxorubicin HCl using spectrophotometry	27
2.4.2	Calibration curve of mannose using spectrophotometry	28
2.4.3	Dialysis membrane preparation	28
2.4.4	Preparation of Phosphate buffer (PB)	29
2.4.5	Dialysis membrane method	29
2.5	Anticancer activity	30
2.5.1	Cell line	30
2.5.2	Cell culture	30
2.5.3	Cytotoxicity test	30
2.5.4	Mannose receptor selectivity test	31
	Chapter Three: Results and Discussion	32
3.1	Synthesis and functionalization of SWCNTs	32
3.2	Characterization of Dox-SWCNTs and Dox-mannose-SWCNTs	36
3.2.1	Dispersibility of the functionalized SWCNTs	36
3.2.2	Morphology and size of the functionalized SWCNTs	37
3.2.3	UV-vis spectrophotometry	38
3.2.4	Thermogravimetric analysis (TGA)	39
3.3	In vitro drug release	40
3.4	Anticancer activity	42
	Conclusion	49
	References	50
	Appendix I	58
	المُلخَص	b

List of Tables

NO	Table Title	Page
3.1	Cumulative release data of Dox from <i>f</i> -SWCNT (7) and <i>f</i> -SWCNTs (11) at pH 7.4 and pH 5.5.	41

List of Figures

NO.	Figure title	Page
1.1	Metastatic process.	1
1.2	Schematic representation showed enhanced permeability and retention effect.	2
1.3	Allotropes of carbon.	5
1.4	Main CNTs functionalization methods.	6
1.5	Non-covalent functionalization of CNTs with pyrene functionalized neoglycolipids.	8
1.6	Covalent functionalization of carbon nanotubes.	9
1.7	Doxorubicin intercalation into DNA.	11
1.8	Chemical structure of Doxorubicin.	12
3.1	Photograph of dispersions of (a) <i>p</i> -SWCNTs, and (b) Dox-SWCNTs (7) and (c) Dox-mannose-SWCNTs (11).	36
3.2	TEM images of (A) pristine SWCNTs; (B) <i>f</i> -SWCNTs (7); (C) <i>f</i> -SWCNTs (11).	37
3.3	Calibration curve of Dox.	38
3.4	Calibration curve of Mannose.	39
3.5	TGA results of <i>p</i> -SWCNTs, <i>f</i> -SWCNTs (7), <i>f</i> -SWCNTS (11).	40
3.6	<i>In vitro</i> release of Dox from A) <i>f</i> -SWCNT (7); B) <i>f</i> -SWCNTs (11) at pH 7.4 and pH 5.5.	42
3.7	Concentration-dependent effect on cell viability (HepG2 cell) at different pH values. (n=6, *p<0.05, compared to 0.0 mcg/ml).	44
3.8	Concentration-dependent effect on cell viability (MCF-7 cell) at different pH values. (n=6, *p<0.05, compared to 0.0 mcg/ml).	45
3.9	pH-dependent effect for 4 mcg/ml of each of the test substance on cell viability of HepG2 cells at different pH values. (n=6, *p<0.05, compared to control).	46
3.10	pH-dependent effect for 4 mcg/ml of each of the test substance on cell viability of MCF-7 cells at different pH values. (n=6, *p<0.05, compared to control).	46
3.11	Effect of pre-incubation with mannose on the cytotoxicity of different test substances in HepG2 cell line at a concentration 4 mcg/ml and a pH of 6.5 (n=3, *p<0.05, compared to 0 μ M mannose).	47
3.12	Effect of pre-incubation with mannose on the cytotoxicity of different test substances in MCF-7 cell line at a concentration 4 mcg/ml and a pH of 6.5 (n=3, *p<0.05, compared to 0 μ M mannose).	48

List of Schemes

NO.	Scheme Title	Page
1	The dual functionalization of SWCNTs with Dox and mannose.	14
2	Covalent functionalization of SWCNTs with Dox.	16
3	Dual functionalization of SWCNTs with Dox and mannose.	16
4	Synthesis of linker (4) .	32
5	Functionalization of SWCNTs with Dox (7) .	33
6	Reduction of 4-nitrophenyl α -D-mannopyranoside.	34
7	Dual functionalization of SWCNTs to obtain the <i>f</i> -SWCNTs (10) .	35
8	Synthesis of <i>f</i> -SWCNTs (11) with Dox.	35

List of abbreviations

Symbol	Abbreviation
A-549	Human lung adenocarcinoma
Anhydrous CuSO ₄	Anhydrous copper sulfate
CDCl ₃	Deuteriochloroform
CGM	Culture growth medium
CHCl ₃	Chloroform
CNTs	Carbon nanotubes
DCM	Dichloromethane
DDs	Drug delivery systems
DMF	Dimethylformamide
DMSO	Dimethylsulfoxide
DNA	Deoxyribonucleic acid
DOX	Doxorubicin
EDC	Ethylcarbodiimide hydrochloride
EDTA	Ethylene diamine tetra acetic acid
EPR	Enhanced permeability and retention
Et ₃ N	Trimethylamine
FBS	Fetal bovine serum
<i>f</i> -MWCNTs	Functionalized multi-walled Carbon Nanotube
<i>f</i> -SWCNTs	Functionalized single-walled Carbon Nanotube
Hr/s	Hour or Hours
H ₂	Hydrogen gas
H ₂ O	Water
HCl	Hydrochloride
HepG-2	Hepatocellular carcinoma
MCF-7	Human breast cancer cell line
MeOD	Deuteromethanol
MeOH	Methanol
Min	Minutes
MTS	(3-(4,5-dimethylthiazol-2-yl)-5-(3-carboxymethoxyphenyl)-2-(4-sulfophenyl)-2H-tetrazolium)
MW	Molecular weight
MWCNT	Multi-walled carbon nanotube
NIR	Near infrared
NMR	Nuclear Magnetic Resonance
°C	Degree Celsius
o-DCB	Ortho dichlorobenzene
PB	Phosphate buffer
PBS	Phosphate buffer saline

Pd/C	Palladium on carbon
PEG	Polyethylene-glycol
pH	Power of hydrogen
<i>p</i> -SWCNTs	Pristine single-walled Carbon Nanotubes
PNPs	Polymeric nanoparticles
QD	Quantum dots
RPMI	Roswell Park Memorial Institute
SWCNT	Single-walled Carbon Nanotube
TEG	Tetraethylene glycol
TEM	Transmission electron microscope
TFA	Trifluoroacetic acid
TGA	Thermogravimetric analysis
THF	Tetrahydrofuran
TLC	Thin layer chromatography
UV-Vis	Ultraviolet-Visible
λ_{\max}	Lambda max

**Dual functionalization of single-walled carbon nanotubes for targeted
cancer therapy**

By

Safa' Raed Dayyeh

Supervisor

Dr. Mohyeddin Assali

Co-Supervisor

Dr. Naim Kittana

Abstract

Chemotherapy is a mainstay strategy in the management of cancer. Regrettably, they suffer from serious side effects due to their effect on healthy cells besides cancerous cells. Therefore, many researchers are eager to develop new drug delivery systems that may help to decrease the side effects and the effective dose of the drug in addition to target delivery of the chemotherapy to cancer cells. One of the epochal drug delivery systems in this field are based on carbon nanotubes technology.

The aim of this work is the covalent functionalization of single walled carbon nanotubes with Doxorubicin in the presence of tetraethylene glycol linker to improve the solubility and dispersibility of the developed nano-drug. Moreover, in order to target the cancer cells, a targeting agent mannose was also loaded on the nano-system. The characterization of the developed nano-drug by transmission electron microscopy showed good dispersibility of the functionalized single walled carbon nanotubes with diameters (6-10) nm. Moreover, the percentage of functionalization was

determined by thermogravimetric analysis showing 25% of functionalization in the case of Dox-SWCNTs (**7**) and 51% for Dox-mannose-SWCNTs (**11**). The *in vitro* release profile of Dox from Dox-SWCNTs (**7**) showed 45% of the loaded drug was released over 18 hr at pH 7.4 and almost complete release at pH 5.5 at 37 °C. However, the *in vitro* release profile of Dox from Dox-mannose-SWCNTs (**11**) showed 75% of the loaded drug was released over 5hr at pH 5.5 at 37 °C.

The cytotoxicity effect of the compounds was studied at different concentrations and different pH conditions and compared with Dox alone. The maximum cytotoxicity effect was observed at 4µg/ml and at pH 6.5. After that, the pre-incubation with any of the tested concentrations of mannose reduced the cytotoxicity of Dox-mannose-SWCNT by approximately 40-57%, suggesting that the entry of this complex might be dependent on mannose receptors, which imparts this complex a kind of selectivity for cancer cells that overexpress this type of receptors.

Chapter one

Introduction

1.1 Cancer

Cancer is a general term for a large group of diseases characterized by the growth of abnormal cells beyond their usual boundaries that can pervade contiguous parts of the body and/or fulminate to other organs. It is the second cause of death globally and accounted for 8.8 million death in 2015 [1].

Cancer cells (or called tumors) have specific capacity to invade and destroy the implied mesenchyme local infestation. These cells need nutrients that are provided through the blood stream in normal tissues. The process of cancer development and induction is called carcinogenesis. This process is a multistage process that is characterized by rapid creation of abnormal cells and can then invade neighboring parts of the body and spread to other organs which is called metastasis [2], figure 1.1.

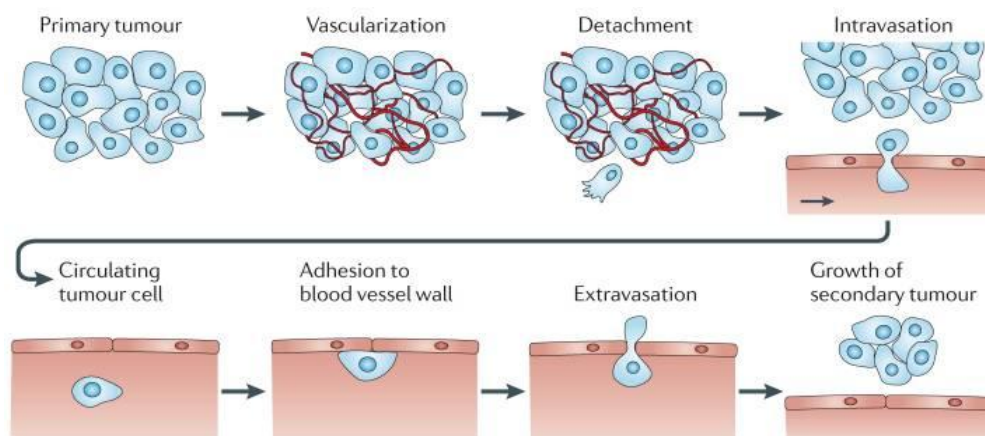


Figure 1.1: metastatic process [3].

Growth of the vascular network is important for the metastatic spread of cancer tissue. The process whereby new blood vessels form is called angiogenesis. Angiogenesis plays an important role in the advancement of cancer by supplying nutrients, oxygen and immune cells as well as removal of waste products [4]. The blood vessels of tumor cells are different from that of normal blood vessels. They are immature, have loose structure, abnormal in the vascular wall, proliferate more rapidly and the endothelial cells lining are discontinuous [5-7]. These differences retained to the phenomenon named as enhanced permeability and retention effect (EPR), figure 1.2. This effect results in spacious leakage of blood plasma components like macromolecules, nanoparticles and lipid particles into the cancerous cells. Furthermore, the slow venous return in cancer cells and the poor lymphatic clearance imply that macromolecules are retained in the cancer cell, while extravasation into cancer cell interstitium continues [8].

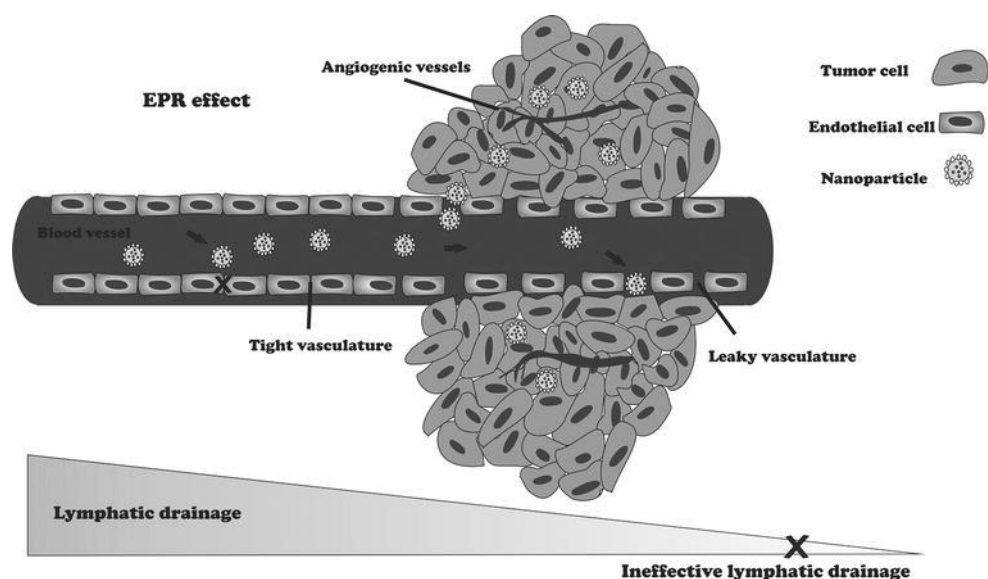


Figure 1.2: schematic representation showed enhanced permeability and retention effect [9].

There are different intervention strategies of cancer treatment include surgery, radiotherapy, chemotherapy, targeted therapy, immunotherapy, and other types of therapies [10-12]. Chemotherapy is the most common intervention that has been recently used. It is usually used to cure the cancer or decrease the symptoms and prevent the spreading of cancer. However, chemotherapy can cause serious side effects including damages of the nerves, deficiency in the immune system, bleeding, dry mouth, stomach upset, vomiting, diarrhea and hair loss [13]. Recently, a novel interventional approach has been introduced to reduce these side effects. This method is based on nano-pharmaceutical technology such as nanoparticles and liposomes. These drug delivery systems (DDS) were developed to deliver the chemotherapeutic drugs by taking advantage of EPR effect in the tumors and this is called passive drug targeting [14].

Another type of drug targeting is active targeting owing to the presence of different ligands on the surface of nano-carriers such as peptides, antibodies, nucleic acids and sugars [15].

Tumor cells have unique properties such as some receptors that are over-expressed on their surfaces, thus differentiate them from the normal cells at molecular level. Attachment of the complementary ligands on the surface of nanoparticles makes them able to target only the cancerous cells [16]. In addition, some tumors of varied origins show marked sugars avidity and high rates of aerobic glycolysis [17]. Therefore, these cancer cells overexpress one or more isoforms of carbohydrates transporters to endure

their growth and survival. A typical glycosylation in the cell membrane in some types of cancer cells results in overexpression of lectin-like receptors that have high affinity for polysaccharides moieties such as mannose, galactose, fructose and lactose [18]. The overexpression of these transporters in tumor cells has been exploited to target cancer cells selectively by conjugating cytotoxic drugs to the sugar of interest for example, Con A is expressed on the surface of a human breast cancerous cell line (MCF-7) has strong binding affinity toward mannose [19, 20]. Another examples on cell line that express mannose receptor are human lung adenocarcinoma (A549) and hepatocellular carcinoma (HepG-2) [21]. Moreover, the increased in aerobic glycolysis in tumor cells leads to lower extracellular and intracellular pH of cancer cells than that normal cells [22]. The mechanism of that is tumors synthesizes ATP by oxidative metabolism and some by glycolytic metabolism (aerobic glycolysis) if the oxygen supply is removed. Due to the disorganized vasculature of tumor and poor lymphatic drainage, pauper clearance of lactic acid could be occur leads to lower intracellular pH. On the other hand, increased H^+ export due to increased functional expression H^+ - pumping ATPases or via activation of Na^+/H^+ exchanger lead indirectly to increase extracellular acidity [23].

Many types of nanomaterials were designed and prepared in order to be applied to medicine including quantum dots (QDs), graphene, magnetic nanoparticles, biodegradable polymeric NPs (PNPs), liposomes, micelles, dendrimers, fullerene, carbon nanotubes (CNTs).

One of the most amazing nanomaterial is CNTs. CNTs have attracted particular concern as transporter of biologically pertinent molecules because of their exclusive chemical, physical and physiological characteristics [24].

1.2 Carbon nanotubes (CNTs)

CNTs are allotropic form of carbon, figure 1.3 [25]. They are structurally described as sheets of six-membered carbon atom rings (like graphene sheet) rolled up into cylinders, needle-like structure so have the tendency to penetrate cellular membranes. CNTs have small size (nanometers in diameter and micrometers in length) so they can enter or adhere to cell surface and can be used as a targeted drug delivery systems [26, 27].

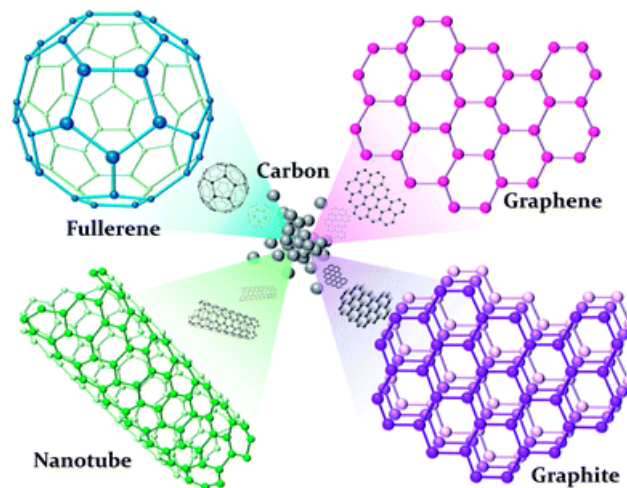


Figure 1.3: Allotropes of carbon [25].

CNTs are divided into two types depending on the number of layers that consists the CNTs: single walled carbon nanotubes (SWNTs) and those with two or more layers are known as multi walled CNTs (MWNTs) [28].

CNTs have limited application in medicine because of their low solubility and high toxicity [29]. Therefore, it is necessary to modify their surface character through functionalization in order to improve their solubility and to provide an opportunity for the fabrication of novel nano drug delivery system [30].

1.3 Functionalization of CNTs:

In order to solve the problem of low water solubility and the formation of complex and entangled bundles of the CNTs, continuous efforts have been made toward that. The functionalization of CNTs is one of the approaches for the modification of CNTs. The most common types are covalent and non-covalent functionalization, figure 1.4 [30]. Adding functional groups alongside the surface and on the defected sites of the nanotubes would increase the water solubility, enhance the biocompatibility and consequently decrease their toxicity [31].

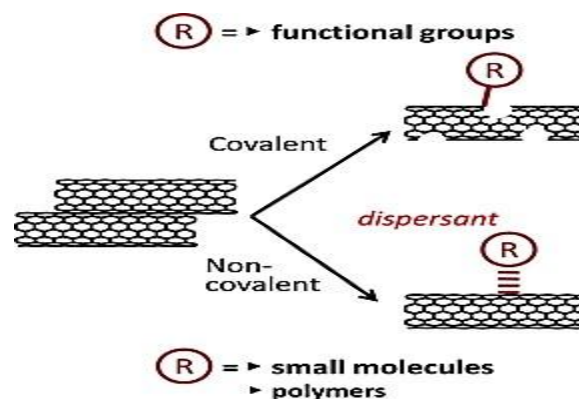


Figure 1.4: Main CNTs functionalization methods [32].

1.3.1 Non-covalent functionalization:

This type of functionalization occurs due to Van der Waals interaction between carbon nanotubes and molecules. For example, aromatic compounds, polymers, and surfactants can be used to modulate the nanotubes surface [33-35]. The obtained non-covalent functionalization maintains the electric properties of CNTs, but remain sensitive to environmental conditions such as pH and salt concentration. Accordingly, the release of the drugs that were charged on the surface of CNTs may occur before reaching the target site [36]. Therefore, using aromatic compounds that interact with the surface of CNTs *via* π - π stacking interactions was evaluated [37-39]. In this manner, Assali *et al.* have developed a new approach for increasing the biocompatibility of nanomaterials through non-covalent functionalization of the surface of CNTs with neoglycolipid compound by π - π stacking interactions, figure 1.5. They synthesized neo-glyco-conjugates structure (compound I) which is a pyrene tail bonded to the glycol-ligand (sugar head) through as spacer, tetra ethylene glycol for better hydrophilic/hydrophobic balance. These aggregates are able to attract specific ligand-lectin interactions similar to glycol conjugates on the cell membrane [40].

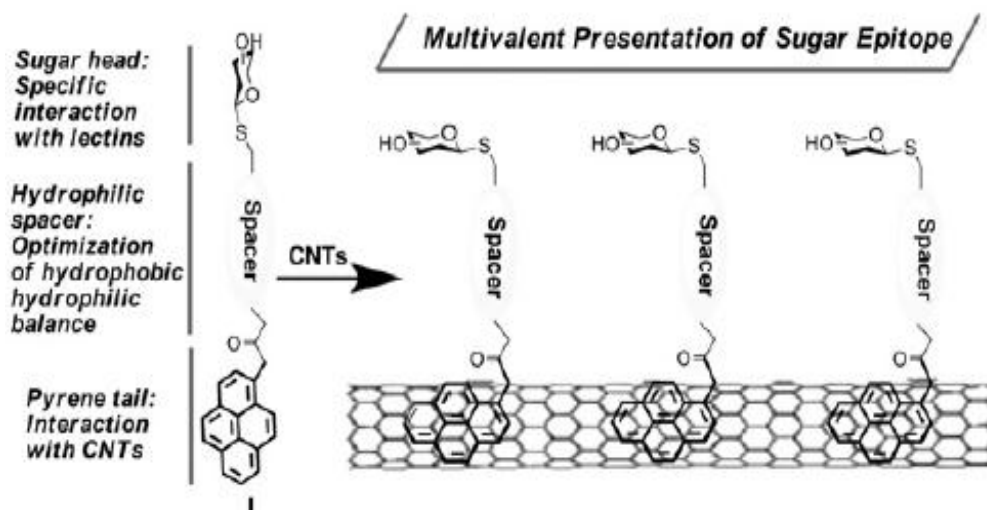


Figure 1.5: Non covalent functionalization of CNTs with pyrene functionalized neoglycolipids [40].

1.3.2 Covalent functionalization:

Covalent chemical modification can be achieved through oxidation reaction [41], arylation [42], addition reactions and other reactions which involve other reactive species, figure 1.6 [30, 43]. Covalent functionalization changes the electrical properties of the CNTs due to change of carbon hybridization from sp^2 to sp^3 . The aim of this type of functionalization is to prevent the release of the attached biomolecules before reaching the target site and consequently decreases the side effects of these biomolecules [44, 45]. This following section, the oxidation functionalization and the addition reaction will be discussed as they used in the thesis.

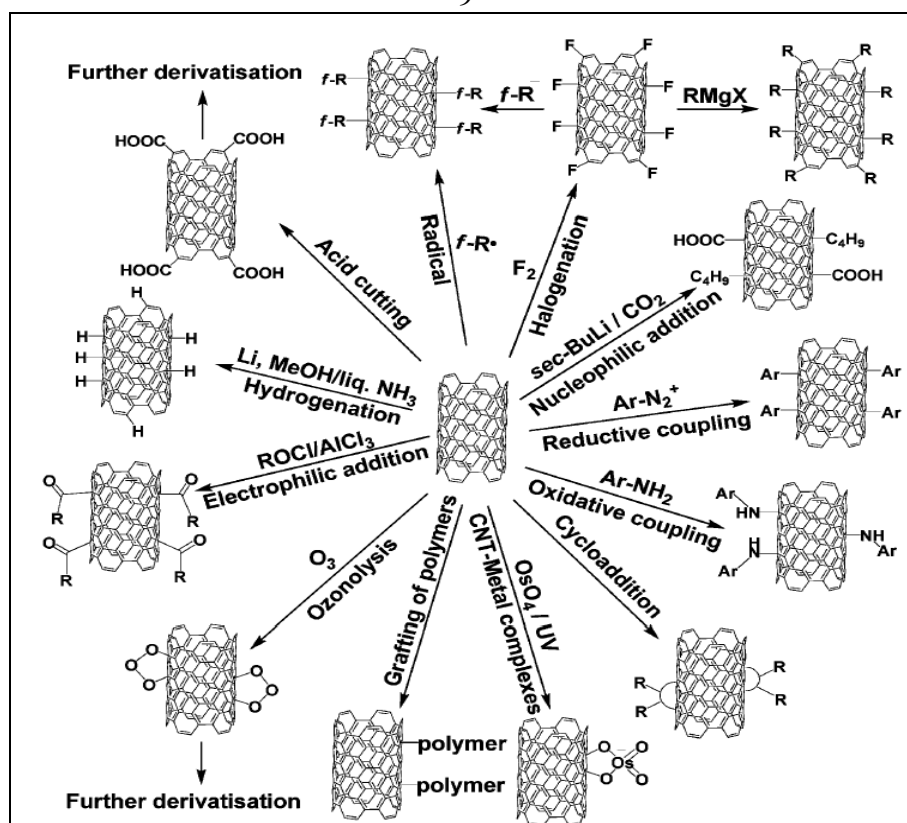


Figure 1.6: Covalent functionalization of carbon nanotubes [30].

1.3.2.1 Oxidation reaction

The oxidation of CNTs occurs in strong acidic and oxidative conditions, such as mixtures of strong acids incorporated with heating or sonication that allowed shortened open tubes decorated with oxygenated functions, predominant on the tips. Among the groups introduced on it, for example (carboxyl, carbonyl, hydroxyl, etc.), the functions are particularly exploited as anchor points for esterification and amidation reactions [44].

1.3.2.2 Addition reaction

This reaction causes functionalization of carbon nanotubes by change the hybridization of carbon atom from sp^2 to sp^3 . These changes are associated

with the modification of the predominantly trigonal-planer local bonding geometry into a tetrahedral geometry. There are different types of addition reactions such as fluorination, cycloaddition, radical additions, nucleophilic and electrophilic additions [44].

Tour and co-workers functionalized SWCNTs with reduced aryl diazonium salts *via* electrochemical reaction. The aryl radicals were generated from the diazonium salts by one-electron reduction [42]. The obtained materials showed good-dispersibility in both organic and water solvents [46].

1.4 Doxorubicin

Doxorubicin (DOX) is a cytotoxic anthracycline antibiotic isolated from cultures of *Streptomyces peucetius* with a molecular weight 580 and a molecular formula $C_{27}H_{30}ClNO_{11}$ [47, 48]. Doxorubicin is an orange red hygroscopic and crystalline powder. It is soluble in water and slightly soluble in methanol [48]. Doxorubicin is one of DNA intercalating agents, used as chemotherapeutic agents. The mechanism of action is through the formation of a cleavable complex of topoisomerase II, subsequently prevents the ligation of the nucleotide strand after double strand breakage resulting in apoptosis, figure 1.7 [49-51].

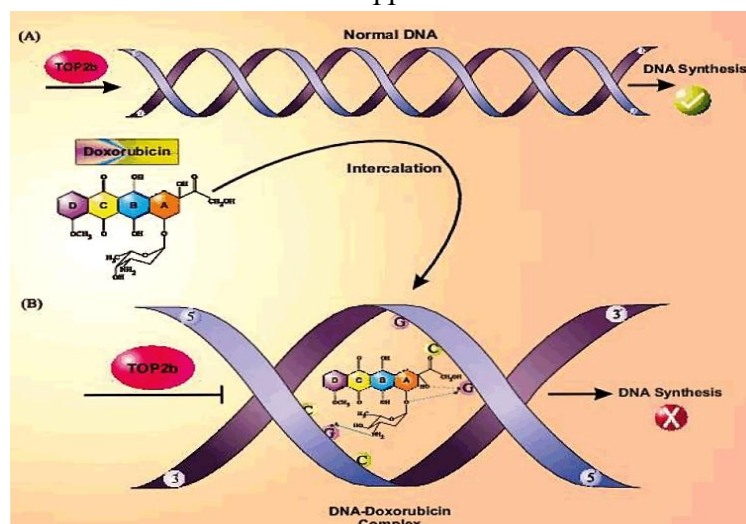


Figure 1.7: Doxorubicin intercalation into DNA. A) Topoisomerase II (TOP2b) relaxes DNA supercoil to facilitate replication and DNA synthesis, B) doxorubicin forms a complex by DNA through G bases in both of DNA strands and prevents TOP2b activity and DNA synthesis.

DOX is indicated in the treatment of a broad spectrum of solid tumors such as bladder, thyroid, stomach, endometrium, breast, ovary and sarcomas of the bone. Also, it can be used in the treatment of lymphoma, as well as acute lymphoblastic and myeloblastic leukemia's [49]. However, the use of DOX is decreased due to series side effects include gastrointestinal disorders, alopecia, stomatitis, bone marrow toxicity and cumulative cardiotoxicity [52].

As mentioned early, the pH value of solid tumors is dropped significantly from 7.2-7.4 to 4.0-6.5 in the intracellular compartment [53]. Therefore, this feature can be used for intracellular drug delivery system by coupling drug to carrier through acid sensitive bond. According to the chemical structure of doxorubicin, figure 1.8, the drug can be designed as prodrug, due to the presence of 3`amino group of sugar moiety and the C-13-keto position [52].

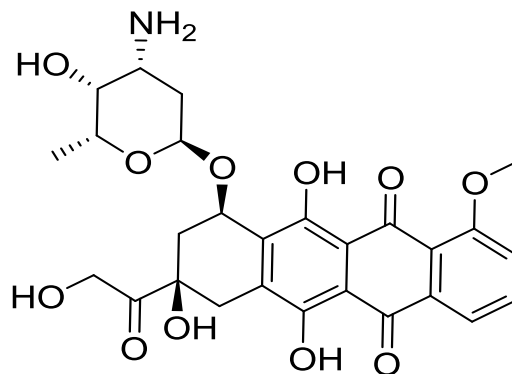


Figure 1.8: Chemical structure of Doxorubicin.

To decrease the side effects and toxicity of the drug, the drug must be more concentrated in the tumor cells. A carrier system can improve the water solubility of a drug, its bioavailability and maintain the tumor inhibition effect with minimum side effects through the utilization of specific targeting agent. This project is focusing on the development of new nano anticancer therapy through the covalent functionalization of carbon nanotube with DOX. Furthermore, in order to decrease the side effects of the drug and to increase its selectivity on the tumor cells, a specific targeting agent like mannose will be connected to the nano-system.

1.5 Literature Review

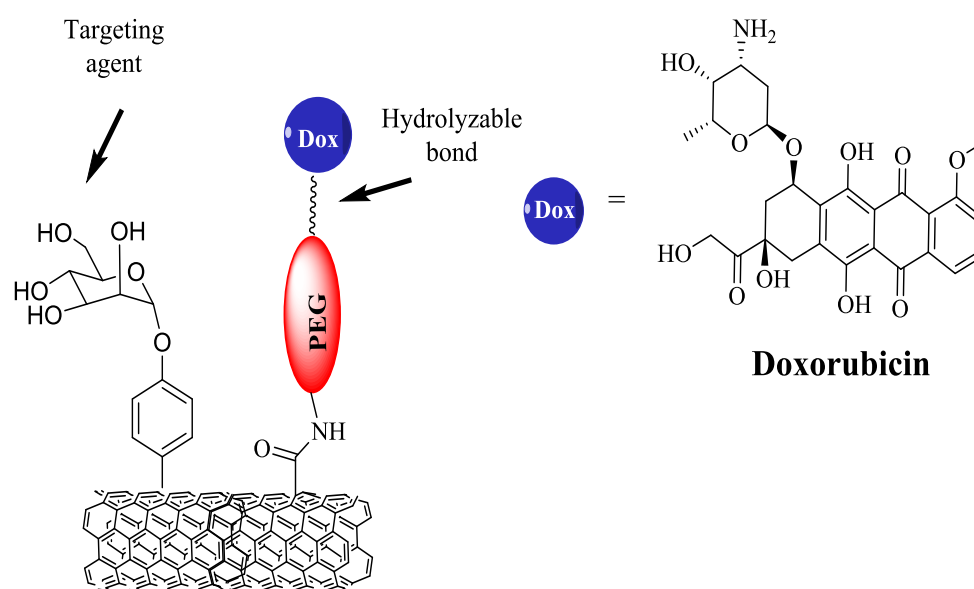
Many attempts were carried out in order to improve the efficacy and safety of the anticancer agents using different types of nano-systems such as nanoparticles, liposomes, micelles and others. In this literature review, DOX conjugated with nanomaterials were mainly reported.

In 2010, You and co-workers developed gold nanospheres capable of mediating both photothermal ablation of cancer cells and DOX release

upon near-infrared (NIR) light irradiation. Irradiation with NIR laser induced photothermal conversion, which triggered rapid DOX release from DOX-loaded gold nanospheres. The study showed that the release of DOX was pH-dependent, with more DOX released in aqueous solution at lower pH [54]. In another study, controlled release and targeted delivery to cancer cells of Dox from polysaccharide functionalized SWCNTs was developed by Yunfei et.al [55]. The obtained system was sonicated in aqueous solutions of the chitosan leading to non-covalent encapsulation of SWCNTs by chitosan. Subsequently, Dox in aqueous solution was attached to the modified SWCNTs by mixing with the chitosan modified SWCNTs. The in vitro studies showed greater cytotoxicity against Hela cells than Dox or SWCNTs alone and this exhibited that the system had controlled and sustained release properties which increase the Dox release [55]. In 2011, pH responsive SWCNTs-Dox complexes in cancer cells was developed and evaluated by Yan-Juan Gu and co-workers. This controlled drug delivery system based on SWCNTs coated with Dox via acid sensitive hydrazone bond. The resulting bond are acid cleavable, which provide a strong pH responsive drug release, thereby expedite Dox release near the acidic tumor microenvironment and thus reduce its overall systemic cytotoxicity. The result showed that the system exhibited high intracellular Dox release thus providing greater cytotoxicity against HepG2 and Hella cells [56].

1.6 Aims of the study

The aim of our study is to develop a new nano-anticancer system based on covalent functionalization of SWCNTs with Dox through acid cleavable bond. Moreover, in order to develop a targeted nano anticancer system, mannose was introduced through the dual functionalization of SWCNTs as shown in the scheme 1:



Scheme 1. The dual functionalization of SWCNTs with Dox and mannose.

1.7 Objectives

- 1) The covalent functionalization of the CNTs in order to load the maximum possible quantity of the anticancer drug.
- 2) Bi-functionalization of CNTs with both the targeting agent and the anticancer drug (Dox).

3) Characterization of the formed nano-anticancer drug by the different analytical techniques such as NMR, UV-Vis spectroscopes, TEM and TGA.

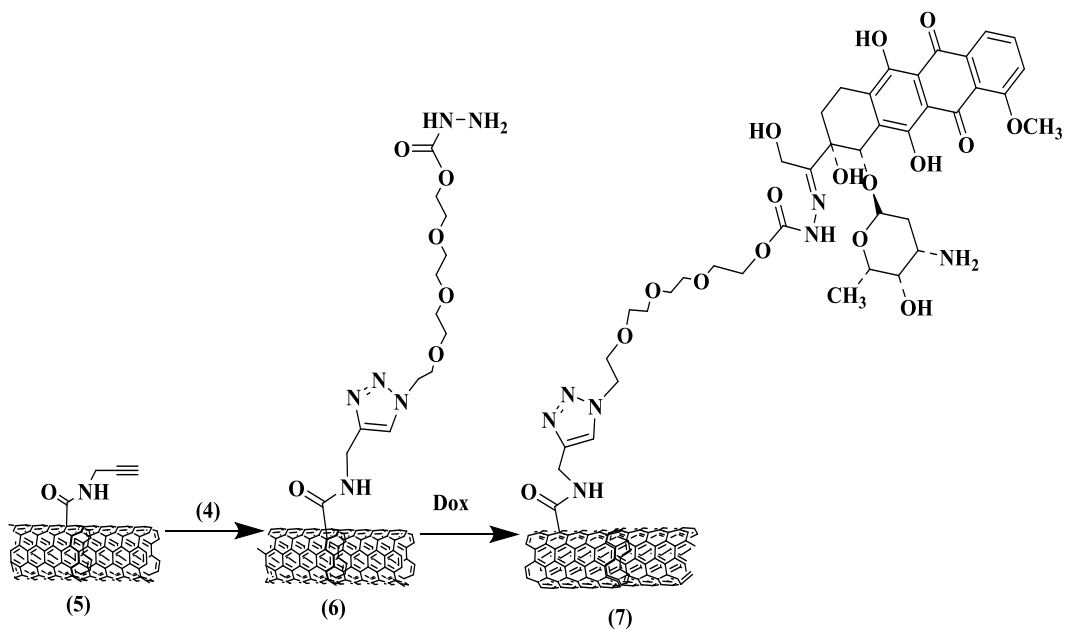
4) In vitro drug release through dialysis membrane.

5) The determination of the anticancer activity by in vitro test and the comparison with the Dox alone.

These objectives aim to develop a new and effective targeted nano-anticancer drug.

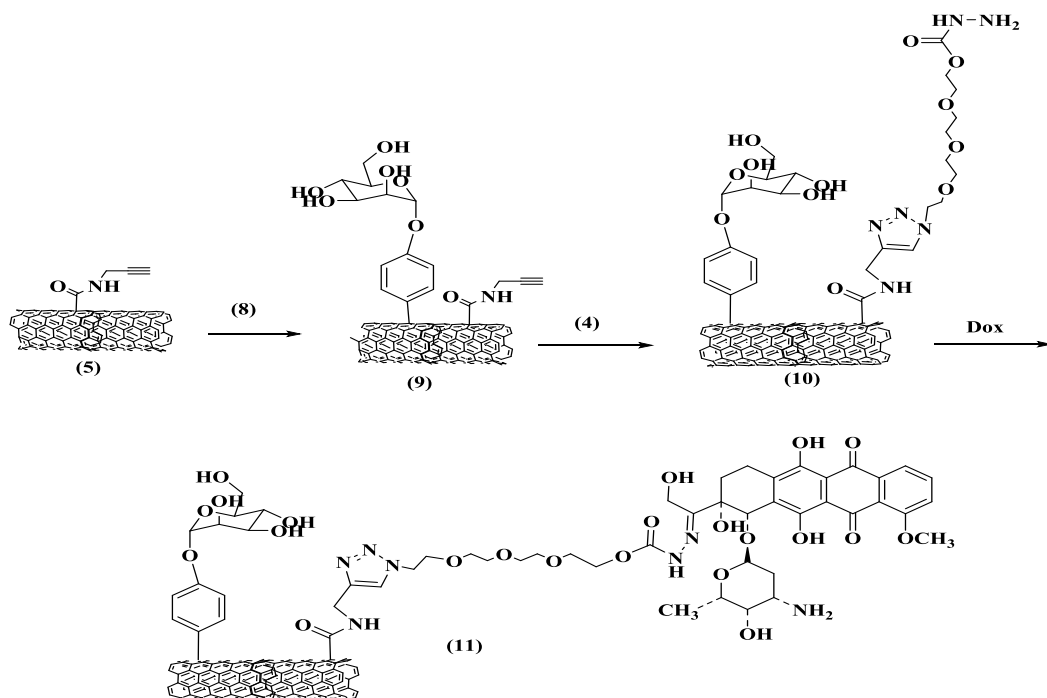
1.8 General approach of the synthesis and functionalization of SWCNTs

Schemes 2 and 3 summarize the functionalization of SWCNTs covalently with doxorubicin and the dual functionalization of SWCNTs with doxorubicin and mannose, respectively. In scheme 2 doxorubicin is attached through hydrolysable linkage to the covalently functionalized SWCNTs.



Scheme 2. Covalent functionalization of SWCNTs with Dox.

Schemes 3 shows the dual functionalization; mannose will be attached to the *f*-SWCNTs through Tour reaction and Dox will be linked through the hydrolysable link as described previously in scheme 2.



Scheme 3. Dual functionalization of SWCNTs with DOX and mannose.

Chapter Two

Methodology

2.1 Reagents and materials

L-ascorbic acid sodium salt (catalog # A17759), 1-(3-Dimethylaminopropyl)-3-ethylcarbodiimide hydrochloride (EDC) (catalog # A10807), propargylamine (catalog # H53495), 4-nitrophenyl- α -D-mannopyranoside (catalog # N01C012), 4-nitrophenylchloroformate (catalog # 10204524), trifluoroacetic acid (TFA) (catalog # A12198) and tetraethylene glycol (TEG) (catalog # B23990) were purchased from Alfa Aesar company (England).

Hydrazine hydrate (catalog # 43480), sodium azide (catalog # 0E30428) and 1,2-Dichlorobenzene (*o*-DCB) (catalog # 65152) were purchased from Riedel de Haën Company (Germany). Mannose (catalog # SLBH1709V), Doxorubicin HCl (catalog # LRAB2383), toluene-4-sulfonylchloride (catalog # 1234411), palladium on carbon (catalog # 101375286), iso-amyl nitrite (catalog # 110463) and anhydrous copper sulfate (catalog # 451657) were purchased from (Sigma-Aldrich, USA). Acetone, ethanol (EtOH), methanol (MeOH) and dichloromethane (DCM) were purchased from (C.S. Company, Haifa). Chloroform (CHCl₃) (catalog # 67-66-3), triethylamine (Et₃N) (catalog # 40502L05) and diethyl ether (catalog # 38132) were purchased from (Merck Millipore) and tetrahydrofuran (THF) solvent (catalog # 487308) was purchased from (Carlo Erba Company, MI. Italy). N, N-Dimethylformamide (DMF) (catalog # 55145) was purchased from

(Frutarom Laboratory Chemicals). Anthrone, disodium hydrogen phosphate, sodium chloride, sodium hydroxide and potassium dihydrogen phosphate were purchased from (C.S. Company, Israel). Carboxylated SWCNTs (Catalog # 99685-96) was purchased from nanostructured and amorphous materials, Inc USA. PTFE-Filter (Sartouris Stedim Biotech GmbH 37070 Gottingen, Germany).

For biological test, Dulbecco's free Ca^{++} -phosphate buffered saline (REF # 02-023-1A) and L-glutamine solution (REF # 03-020-1B) were purchased from (Biological industries, Jerusalem). RPMI (catalogue # 05669) was purchased from (Manassas, VA, USA), Trypsin-EDTA solution 1X (catalog # 59417C), fetal Bovin Serum (catalog # C8065) and trypan blue solution (catalog RNBD6249) were purchased from (sigma-aldrich, USA). Celltiter 96[®] Aqueous one solution cell proliferation Assay (# G3580, USA).

2.2 Instrumentation

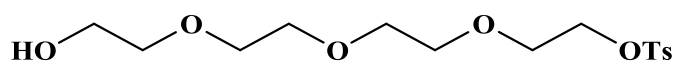
NMR analysis was measured by Bruker Avance 500 spectrometer at Jordan University. Absorption analysis was conducted on (7315 Spectrophotometer, Jenway, UK) using 10-mm quartz cuvettes. Esco celculture CO_2 incubator was used to incubate cell line. Accumax Variable micropipette, UK was used for pipetting. TGA analysis was achieved on STA instrument at Jordan University with a flow rate 20 °C under nitrogen (100 cc/min) with a range 25-600 °C. TEM images were done on FEI Morgagni at Jordan University. FTIR analysis was done on Nicolet iS5,

ThermoFisher Scientific Company, USA. Unilab microplate reader 6000 was used to read the plate for cell viability test.

2.3 Synthesis and characterization of the products:

All the synthetic procedures and anticancer activity were prepared at An-Najah University laboratories. NMR, TEM and TGA measurements were conducted at the University of Jordan.

2.3.1 Synthesis of Tosyl-TEG-OH (1)



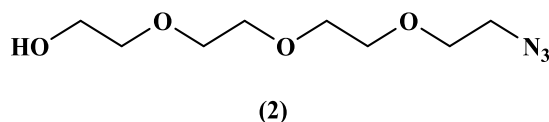
(1)

To a solution of tetraethylene glycol (10 g, 51.5 mmol) and Et_3N (7 ml, 51.5 mmol) in 40 ml THF stirred for 5 min and cooled at 0 °C, tosyl chloride (10 g, 52.5 mmol) was added dropwise over a period of 30 min. The reaction was stirred vigorously overnight at room temperature. The resultant product was diluted by CHCl_3 (200 mL), washed with HCl 1M (50 mL) and brine (50 mL). The solvent was removed under vacuum and the remaining crude was purified by flash chromatography on silica gel, eluting with $\text{CHCl}_3/\text{MeOH}$ (20:1) to give a pale yellow oil. The yield was 36% (4 g, 14.3 mmol).

R_f: 0.5($\text{CHCl}_3/\text{MeOH}$ 9:1)

^1H NMR (400 MHz, CDCl_3): δ 7.77 (d, 2H, $J = 8.3$ Hz, Ts), 7.33 (d, 2H, $J = 8.0$ Hz, Ts), 4.13 (t, 2H, $J = 4.7$ Hz, CH_2OTs), 3.66 (t, 2H, $J = 4.9$ Hz, $\text{CH}_2\text{CH}_2\text{OTs}$), 3.57-3.56 (m, 8H, 4 CH_2O), 3.50 (t, 2H, $J = 5.2$ Hz, $\text{CH}_2\text{CH}_2\text{OH}$), 3.27 (s, 2H, CH_2OH). **^{13}C NMR (100.6 MHz, CDCl_3):** δ 144.8 (2CH Ar), 133.0 (2CH Ar), 129.8 (C Ar), 127.9 (C Ar), 70.7, 70.5, 70.2, 70.1 ($\text{CH}_2\text{CH}_2\text{OH}$), 69.2 (CH_2OTs), 68.6 ($\text{CH}_2\text{CH}_2\text{OTs}$), 40.3 (CH_2OH).

2.3.2 Synthesis of OH-TEG-N3 (2)



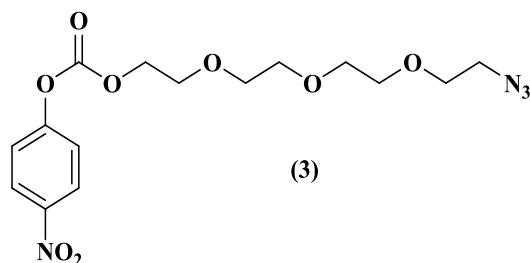
To a solution of compound **1** (1.4g, 4.02 mmol) dissolved in 6 ml EtOH, sodium azide (287.4 mg, 4.42 mmol) was added. The reaction was stirred at 70 °C overnight. After removing of EtOH under vacuum, the reaction was diluted with diethyl ether (100 ml) and washed with brine (40 ml). The solvent was removed under vacuum to give a pale yellow oil product. The obtained yield was 85% (1.23 g, 5.6 mmol).

R_f: 0.39 (DCM/MeOH 20:1)

^1H NMR (500 MHz, CDCl_3): δ 3.58 (t, 2H, $J = 4.8$ Hz, HOCH_2CH_2), 3.55-3.51 (m, 10H, 5 CH_2O), 3.46 (t, 2H, $J = 4.8$ Hz, $\text{OCH}_2\text{CH}_2\text{N}_3$), 3.26 (t, 2H, $J = 4.8$ Hz, $\text{CH}_2\text{CH}_2\text{N}_3$), 3.10 (bs, 1H, OH). **^{13}C NMR (125.7 MHz,**

CDCl_3): δ 72.5 ($\text{HOCH}_2\text{CH}_2\text{O}$), 70.6, 70.5, 70.4, 70.2, 69.9 (CH_2O), 61.5 (COH), 50.5 (CN_3).

2.3.3 Synthesis of N3-TEG-nitrophenyl carbonate (3)



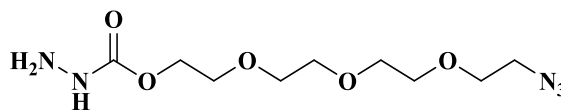
Compound **2** (0.17 g, 0.78 mmol) and Et_3N (21.6 μl , 0.16 mmol) dissolved in 6ml methylene chloride. The reaction was stirred at 0°C for 2 hr under argon. After that, 4-nitrophenyl chloroformate (156.3 mg, 0.78 mmol) dissolved in 7 ml of Methylene chloride was added dropwise to the reaction. The reaction was stirred 24 h under argon. The resultant pale yellow oil product was obtained after removing of solvent under vacuum. (Yield 96%, 0.31 g, 0.81 mmol).

R_f: 0.29, (DCM/MeOH 20:1).

IR: 1767.47, 1616.94, 2114 cm^{-1}

^1H NMR (400 MHz, MeOD): δ 8.12 (d, 2H, $J = 9.1$ Hz, Ar), 6.90 (d, 2H, $J = 9.3$ Hz, Ar), 3.68-3.62 (m, 12H, 6 CH_2O), 3.56 (t, 2H, $J = 5.1$ Hz, $\text{OCH}_2\text{CH}_2\text{N}_3$), 3.38 (t, 2H, $J = 5.1$ Hz, $\text{CH}_2\text{CH}_2\text{N}_3$). **^{13}C NMR (100.6 MHz, MeOD)**: δ 156.0, 152.0, 145.2, 125.6, 115.1, 72.2, 70.2, 70.1, 70.0, 69.9, 69.6, 60.8, 50.3.

2.3.4 Synthesis of hydrazine derivative (4)



(4)

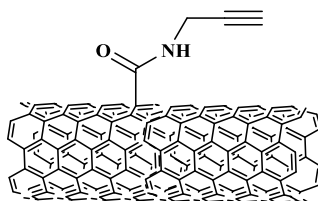
Hydrazine hydrate (2.5 ml, 50.1 mmol) was added to a solution of compound **3** (0.20 g, 0.51 mmol) dissolved in 12 ml methylene chloride. The reaction was stirred at 50°C for 5 hrs. The solution was diluted with (2 x 40 ml) methylene chloride and washed with (30 ml) brine. The reaction was evaporated by rotavapor to give yellowish oil product. (Yield 70%, 0.10 g, 0.36 mmol).

R_f: 0.8 (DCM/MeOH 9:1).

IR: 2944.71, 2914.91, 2104.75, 1722.14 cm⁻¹

¹H NMR (500 MHz, DMSO): δ 8.18 (bs, 1H, NHCO), 5.74 (s, 2H, NH₂), 4.07 (t, 2H, *J* = 4.6 Hz, CH₂OCO), 3.60 (t, 2H, *J* = 4.9 Hz, COOCH₂CH₂O), 3.55-3.47 (m, 10H, 5 CH₂O), 3.39 (t, 2H, *J* = 4.9 Hz, CH₂N₃). **¹³C NMR (125.7 MHz, DMSO)**: δ 155.2, 72.33, 69.87, 69.81, 69.77, 69.71, 69.25, 60.22, 50.01.

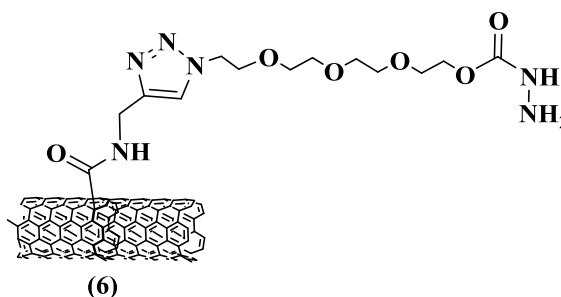
2.3.5 Synthesis of SWCNTs-alkyne (5)



(5)

To carboxylated SWCNTs (75 mg) solubilized in DMF (30 ml). EDC (30.0 mg, 0.16 mmol) and Et₃N (300 μ l, 2.19 mmol) were added. The solution was sonicated for 1hr, then the propargylamine (52 μ l, 0.82 mmol) was added. The reaction was sonicated for 10 min and stirred for 72hr under argon. CHCl₃ (25 ml) was added to reaction, filtered under vacuum with CHCl₃(2 x 20 ml), DCM (10 ml) and diethyl ether (2x 20 ml). The black powder was collected and the obtained weight was 40 mg.

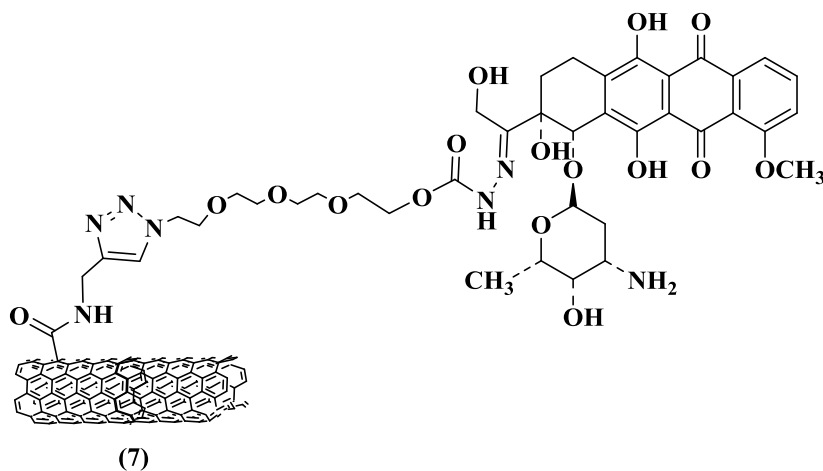
2.3.6 Functionalization of *f*-SWCNTs 5 with compound 4 (6)



A sonicated solution of compound 4 (90 mg, 0.24 mmol) and *f*-SWCNTs 5 (30 mg) dissolved in 4 ml of methylene chloride was added to a solution of anhydrous CuSO₄ (23 mg, 0.15 mmol), L-ascorbic acid Na salt (26 mg, 0.15 mmol) in 4 ml of distilled H₂O. The reaction was stirred for 24hr. The reaction was sonicated after 15 ml of MeOH was added to it. The product was filtered under vacuum and washed with MeOH and ether. The black powder was collected and dried weight was 29 mg.

IR: 2913.98, 2841.16, 1648.22 cm⁻¹

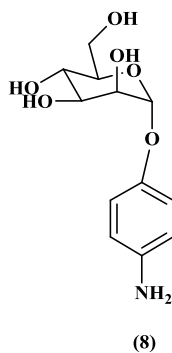
2.3.7 Functionalization of *f*-SWCNTs **6** with Doxorubicin (**7**)



Compound **6** (10 mg) was dispersed in dried MeOH (5ml), Doxorubicin HCl (15 mg) dried under vacuum and 1 drop of trifluoroacetic acid (TFA) was added. The reaction was stirred at room temperature in the dark for 48hr under argon. The resultant product was filtered under vacuum, washed with MeOH, DCM and ether. The black powder was collected and dried weight was 8 mg.

IR: 2917.15, 2837.99, 3740.37, 1577.84 cm^{-1}

2.3.8 Synthesis of 4-aminophenyl α -D-mannopyranoside (**8**)



4-nitrophenyl α -D-mannopyranoside (0.10 g, 0.37 mmol) dissolved in 5 ml Milli Q water, (10 mg) Pd/C was added to it after sonication for 10 min.

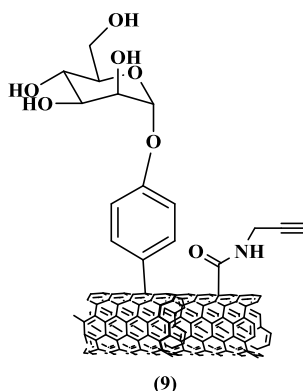
The reaction was stirred at room temperature overnight under H₂ bubbling. The reaction was filtered using silica gel and washed with EtOH. The solvent was removed under vacuum to give yellowish brown sticky product. (Yield 99%, 80 mg, 0.37 mmol).

R_f: 0.25(DCM/MeOH 9:1).

IR: 2939.51, 2851.22, 1649.85, 3319.28 cm⁻¹

¹H NMR (500 MHz, MeOD): δ 6.82 (d, 2H, *J* = 9.2 MHz), 6.55 (d, 2H, *J* = 8.7 MHz), 5.32 (s, 1H; H-1), 3.98 (m, 1H), 3.85 (dd, 1H, *J* = 9.0 MHz, *J* = 2.8 MHz), 3.73 (dd, 1H, *J* = 11.3 MHz, *J* = 2.2 MHz), 3.71-3.73 (m, 2H), 3.62-3.65 (m, 1H); **¹³C NMR (125 MHz, MeOD)**: δ 149.7, 143.1, 118.2, 116.8, 101.0, 74.0, 72.2, 72.0, 67.3, 61.9.

2.3.9 Functionalization of SWCNTs-Alkyne with compound 8 (9)

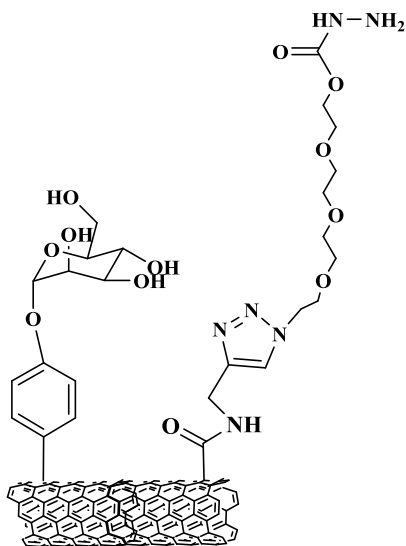


Compound **8** (82 mg, 0.40 mmol) and SWCNTs-alkyne **5** (30 mg) dispersed in *o*-DCB: DMF (2:1, 25 ml) under vacuum and argon. The reaction was sonicated for 30 min under argon bubbling, iso-amyl nitrite (350 μl) was added dropwise to the reaction. The reaction was stirred at

65°C for 24hr under argon. The product was filtered under vacuum, washed with MeOH, acetone and ether to get 57mg of black powder.

IR: 3645.38, 2917.15, 1562.01cm⁻¹

2.3.10 Functionalization of *f*-SWCNTs **9** with compound **4** (**10**)

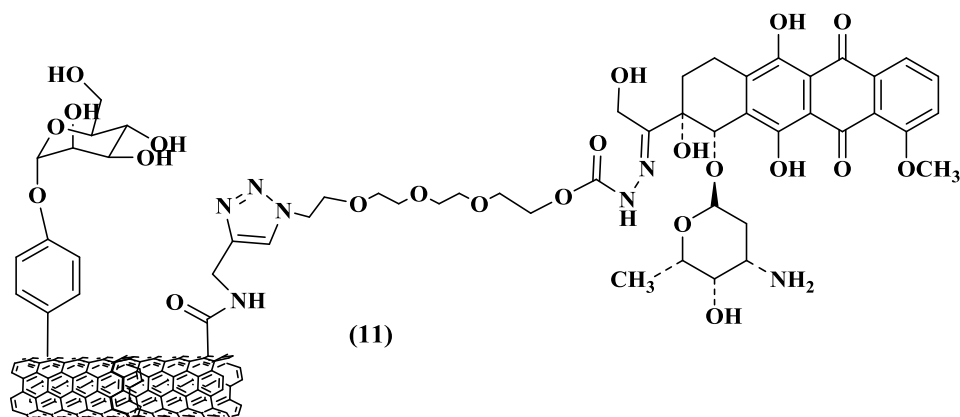


(10)

Compound **4** (90 mg, 0.33 mmol) and *f*-SWCNTs **9** (30 mg) dispersed in 4 ml of DCM was added to a solution of anhydrous CuSO₄ (23 mg, 0.15 mmol), L-ascorbic acid Na salt (26 mg, 0.15 mmol) dissolved in 4 ml of distilled H₂O. The reaction was stirred for 24 hr. The reaction was sonicated after addition of 15 ml of MeOH to it. The product was filtered under vacuum, washed with MeOH and ether. The black powder was collected and the obtained weight was 29 mg.

IR: 3352.67, 2917.15, 2913.98, 1625.33cm⁻¹

2.3.11 Functionalization of *f*-SWCNTs **10** with Doxorubicin (**11**)



Compound **10** (15 mg) was dispersed in dried MeOH (5ml), Doxorubicin HCl (15 mg) dried under vacuum and 1 drop of trifluoroacetic acid (TFA) was added. The reaction was stirred at room temperature in the dark for 48hr under argon. The resultant product was filtered under vacuum, washed with MeOH, DCM and ether. The black powder was collected and dried weight was 14 mg. The amount of mannose was determined by anthrone method. Moreover, the amount of attached DOX was determined through spectrophotometric method.

IR: 3559.89, 2920.32, 2917.15, 1647.49 cm^{-1}

2.4 In vitro drug release

2.4.1 Calibration curve of Doxorubicin HCl using spectrophotometry

A calibration curve of Doxorubicin HCl was prepared at λ_{max} 485 nm using a serial dilutions (0.05, 0.04, 0.03, 0.02 and 0.01 mg/ml) of Doxorubicin (5 mg/5ml) in distilled water. The calibration curve was constructed

by plotting absorbance *vs.* concentration to determine the quantity of the loaded doxorubicin on the surface of the SWCNTs.

2.4.2 Calibration curve of mannose using spectrophotometry

A calibration curve of mannose was prepared at λ_{\max} 620 nm using a serial dilutions (0.05, 0.04, 0.03, 0.02 and 0.01 mg/ml) of mannose (1 mg/ml) in distilled water according to anthrone method.

2.4.2.1 Anthrone method

0.5 ml from a serial dilutions (0.05, 0.04, 0.03, 0.02 and 0.01 mg/ml) of mannose (1 mg/ml) in distilled water was added to 1 ml of (0.2% anthrone in sulfuric acid) at 0°C. After that, the mixture was incubated at 100°C for 10 min. Then, the mixture was transferred to ice until reach the room temperature. After that, the absorbance was measured at λ_{\max} 620 nm. [57, 58].

2.4.3 Dialysis membrane preparation

Drug release was studied using a dialysis method. Dialysis bag (12.000-14.000 MW cut off, Spectrum Laboratories, Inc) was soaked in 1 L of 2% NaHCO₃/1mM EDTA and boiled for 10 min, then rinsed and boiled for 10 min thoroughly with distilled water. Finally, it was submerged completely in 50% EtOH/1mM EDTA to remove the preservatives and stored at 4°C. It was rinsed thoroughly with phosphate buffer before use.

2.4.4 Preparation of Phosphate buffer (PB)

2.4.4.1 Preparation of PB 5.5

Dissolve 13.61g of potassium dihydrogen phosphate in water and dilute it to 1 L (solution A). Dissolve 35.81g of disodium hydrogen phosphate in water and dilute to 1 L with the same solvent (solution B). Mix 96.4 ml of solution A and 3.6 ml of solution B [59].

2.4.4.2 Preparation of PB 7.4

Add 250 ml of 0.2 M potassium dihydrogen phosphate to 393.4 ml of 0.1 M sodium hydroxide [59].

2.4.5 Dialysis membrane method

Two freshly prepared dispersions of *f*-SWCNTs **7** and **11** (5mg/5ml) were prepared using PB at pH 7.4 and at pH 5.5 respectively. 5mg-5ml were transferred to a dialysis bags. The bags are closed at both ends and tested for leakage. Each bag was immersed in 10 ml of the respective buffer solution at (pH 7.4 and pH 5.5) and gently stirred for 18 hr at 37°C. About 2 ml of an aliquot was withdrawn at each of the time periods (30min, 60min, ..., etc.) and was replaced with equal volume maintain the sink conditions.

2.5 Anticancer activity

2.5.1 Cell line

The cytotoxic activity was determined against HepG2 cells and MCF-7 cells in comparison to the free Dox and *f*-SWCNTs with Dox without mannose.

2.5.2 Cell culture

The cells were cultured in 200-cm² flasks supplemented with medium containing RPMI provided with 10% FBS, penicillin/streptomycin and L-glutamine. Cells were stored in incubator at 37°C with 5% CO₂.

For sub-culturing, the medium was suctioned and washed with excess of Ca²⁺-free PBS. After that, 0.025% of trypsin was added to cells, just enough to cover the cells and incubated with trypsin for up to 5 min in the cell culture incubator until sufficient cell detach from the flask. Trypsin was inactivated by 10 ml of CGM, the cell suspension was collected, and the viable cell count was determined using trypan blue stain before adjusting the cell concentration to 50.000 cell/ml. then the cells were seeded in 96-well plate as 5000 cell/well. The cells were left to adhere and accommodate overnight before running any test.

2.5.3 Cytotoxicity test

The cells were sub-cultured in 96 well plates as explained above. A concentration-dependent cytotoxicity experiment was performed for the

test substances for equivalent concentrations of Dox (0.0, 0.5, 1.0, 2.0 and 4.0 $\mu\text{g/ml}$) under different pH conditions (7.4, 7.0 and 6.5), where 100 μl of the test medium was used per well. After overnight incubation with the test conditions, 10 μl of MTS solution was added to each well and incubated for 2hr in cell culture incubator, after which the absorbance was measured at 490 nm by a plate reader.

2.5.4 Mannose receptor selectivity test

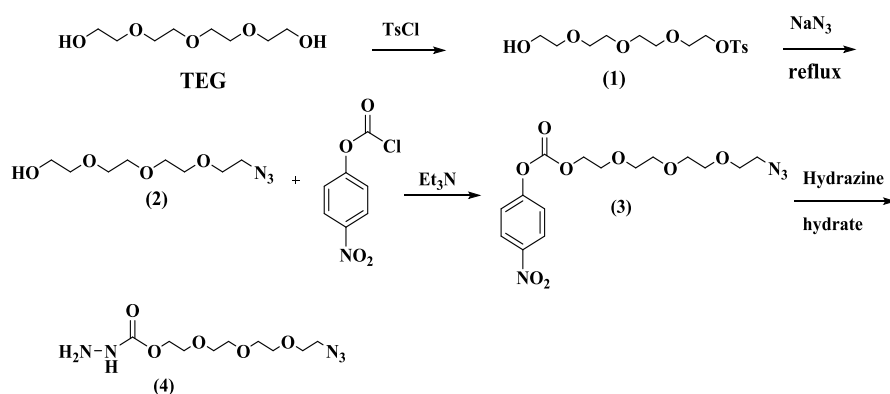
Cells were cultured in 96 well plate as described above were incubated for 30 min with CGM supplemented with different concentrations of mannose (1500 μM , 1000 μM , 500 μM , 0 μM) in a cell culture incubator. After that, the medium was exchanged for CGM containing different concentrations of the test substances at pH 6.5. The cells were incubated for 24hr. After that, MTS test was performed as explained above.

Chapter Three

Results and Discussion

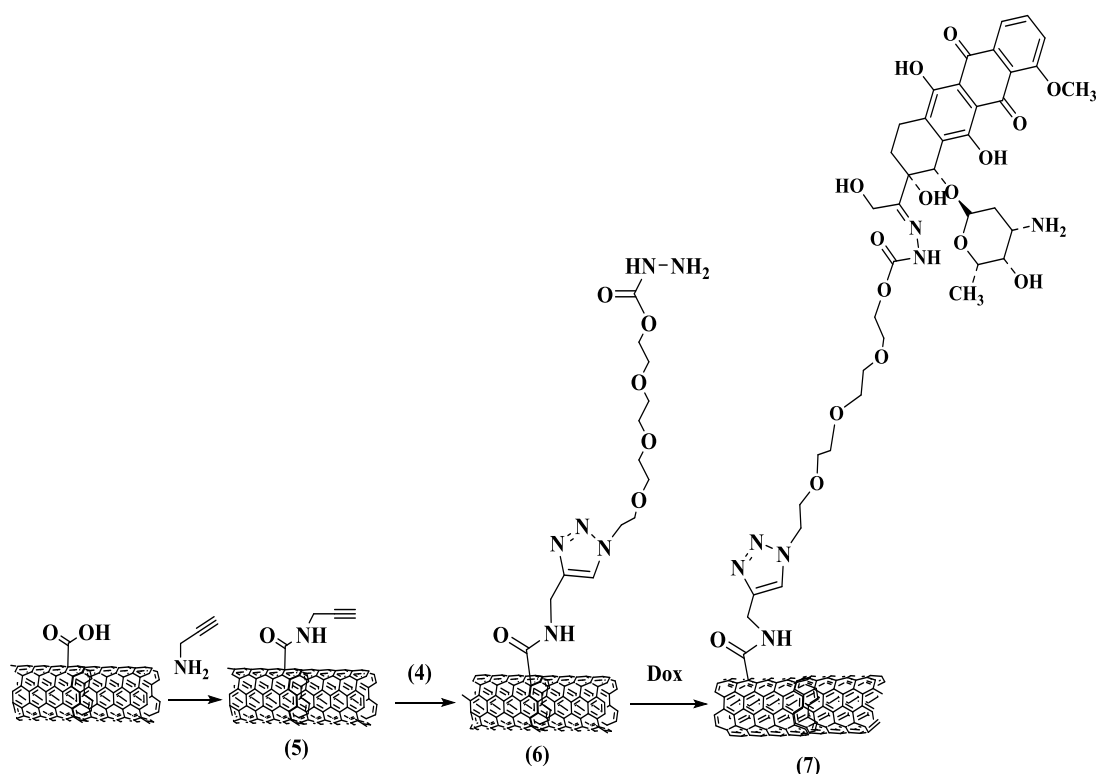
3.1 Synthesis and functionalization of SWCNTs

As one of the main aim of this thesis is the covalent functionalization of SWCNTs with Dox through a hydrolyzable linker that can be cleaved in a mild acidic pH. Herein, a derivative of tetraethylene glycol (TEG) was synthesized using several steps started with the reaction of OH group of TEG with tosyl group to get compound (1). After that, the tosyl group was replaced with azide group through the reaction of (1) with sodium azide in EtOH to get TEG-N₃ (2). Then, compound (2) was reacted with 4-nitrophenyl chloroformate using a catalytic amount of Et₃N to obtain compound (3) with an excellent yield. Finally, the hydrazine bond was formed through reaction between hydrazine hydrate and compound (3) as shown in Scheme 4.



Scheme 4. Synthesis of linker (4).

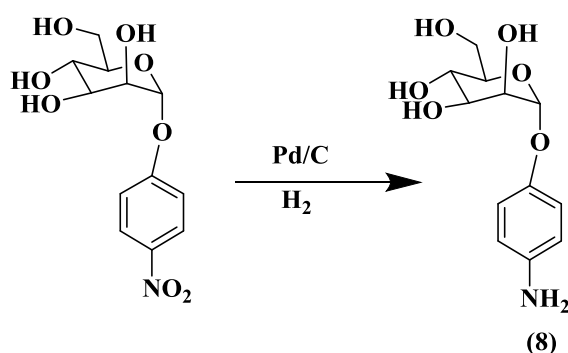
After the successful synthesis of Hydrazine-TEG-N₃ (4), the carboxylated-SWCNTs were functionalized covalently with propargylamine through amidation reaction to get terminal alkyne group SWCNTs (5). After that, *f*-SWCNTs (5) were reacted with compound (4) through click reaction using copper sulfate and ascorbic acid as catalysts to obtain the SWCNTs functionalized with the hydrazine terminal group (6). In a final step and to connect the Dox to the carbon nanotubes, the *f*-SWCNTs (6) were incubated with doxorubicin.HCl for 48 hours in the dark to obtain the monofunctionalized SWCNTs with Dox as shown in scheme 5.



Scheme 5. Functionalization of SWCNTs with Dox.

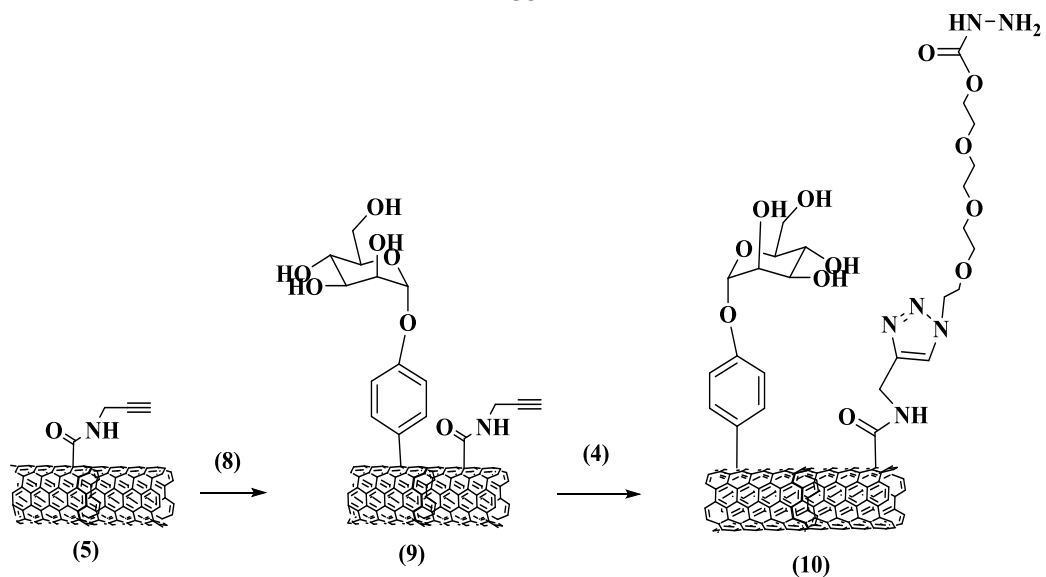
As the monofunctionalization of the SWCNTs with Dox was achieved, the second main aim of this project is the dual functionalization of the SWCNTs with a targeting agent (mannose) in order to specifically

targeting the cancer cells. As we discussed earlier, some cancer cell lines overexpressed mannose receptors on their surface especially hepatic cancer and breast cancer. Therefore and to achieve this aim, 4-nitrophenyl α -D-mannopyranoside was reduced using palladium over carbon as a catalyst in the presence of hydrogen in order to obtain 4-aminophenyl α -D-mannopyranoside (**8**) scheme 6, that can be bind to SWCNTs through Tour reaction.



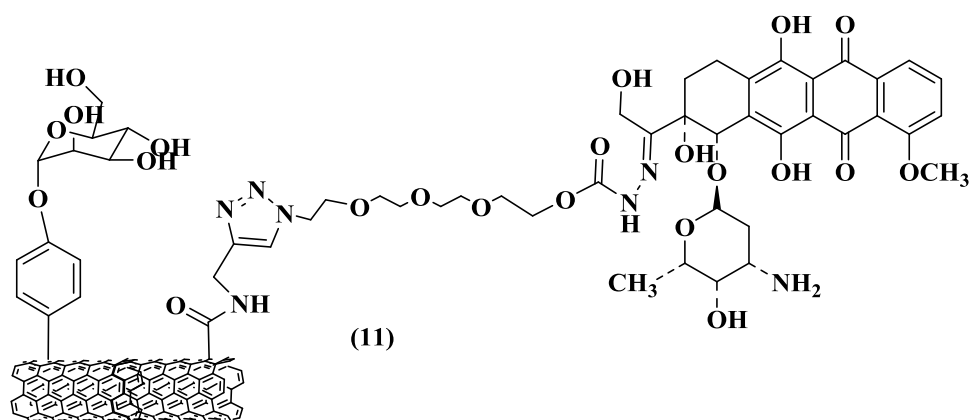
Scheme 6. Reduction of 4-nitrophenyl α -D-mannopyranoside.

The reaction of compound (**8**) with *f*-SWCNTs (**5**) was conducted through Tour reaction by using iso-amyl nitrite as catalyst, which dissolved in *o*-DCB and DMF to obtained (**9**). After that, the *f*-SWCNTs (**9**) were effectively bind with compound (**4**) through click reaction by using anhydrous CuSO₄ and ascorbic acid as catalysts which dissolved in DCM and water to obtain the *f*-SWCNTs (**10**), scheme 7.



Scheme 7. Dual functionalization of SWCNTs to obtain the *f*-SWCNTs (10).

In a final step, the *f*-SWCNTs (10) were incubated with Dox in the presence of a catalytic amount of TFA as a catalyst to obtain the final product (11) as shown in scheme 8.



Scheme 8. Synthesis of *f*-SWCNTs (11) with Dox.

3.2 Characterization of Dox-SWCNTs and Dox-mannose-SWCNTs

3.2.1 Dispersibility of the functionalized SWCNTs

After the functionalization of SWCNTs, the dispersibility of *p*-SWCNTs, Dox-SWCNTs (**7**) and Dox-mannose-SWCNTs (**11**) in water was conducted. The *p*-SWCNTs (**a**) formed a clear black sediment after being suspended in water; while compound **7** (**b**) and **11** (**c**) showed a good water dispersibility, figure 3.1. In fact, the *p*-SWCNTs have hydrophobic characteristics, which persuade the rapid aggregation of these nanotubes. However, the stable black suspensions of compounds (**7**) and (**11**) were due to the increase in the hydrophilicity, which was obtained by the new functionalization of SWCNTs.

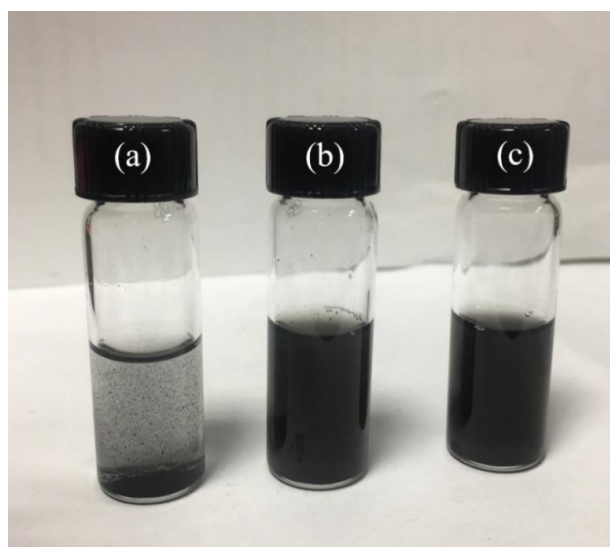


Figure 3.1: Photograph of dispersions of (a) *p*-SWCNTs, and (b) Dox-SWCNTs (**7**) and (c) Dox-mannose-SWCNTs (**11**).

3.2.2 Morphology and size of the functionalized SWCNTs

Beside the macroscopic observation of the successful functionalization of SWCNTs, a microscopic evaluation was conducted by transmission electron microscope (TEM). As mentioned previously, due to the hydrophobic character of the pristine single walled carbon nanotubes, they are found as series of bundles that formed through the Van Der Waals interactions between the nanotubes as shown in figure 3.2A. However, upon the functionalization of these single walled carbon nanotubes and the addition of hydrophilic functional groups, these nanotubes will be dispersed and de-bundled as we can see in figures 3.2B and 3.2C that demonstrate TEM images of *f*-SWCNTs (7) and *f*-SWCNTs (11), respectively. Moreover, the diameters of the observed functionalized SWCNTs were in the range of 6-10 nm in both cases. These observations confirm the dispersability and functionalization of the single walled carbon nanotubes at macroscopic and microscopic levels.

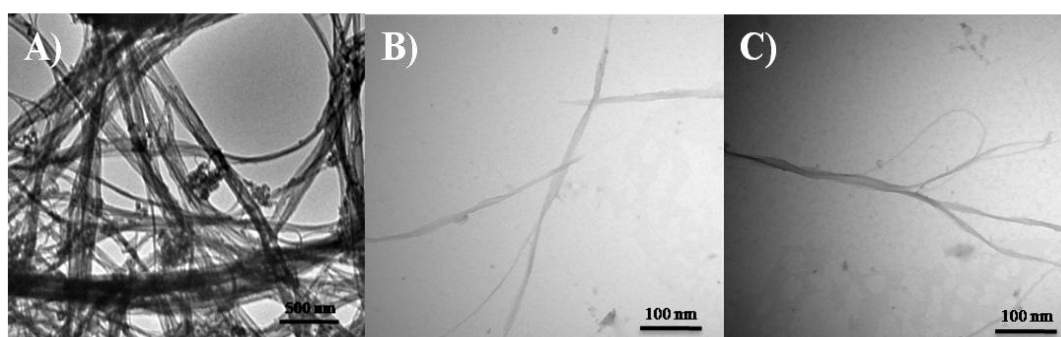


Figure 3.2: TEM images of (A) pristine SWCNTs; (B) *f*-SWCNTs (7); (C) *f*-SWCNTs (11).

3.2.3 UV-vis spectrophotometry

3.2.3.1 Calibration curve of Doxorubicin

The loaded amount of Dox was measured by spectrophotometry. A calibration curve of Dox has been constructed at λ_{\max} 485 nm with a R^2 0.996 as shown in figure 3.3. The loaded amount of Dox on SWCNTs was about 24 μ g/mg of Dox-SWCNTs (7) and 112 μ g/mg of Dox-mannose-SWCNTs (11).

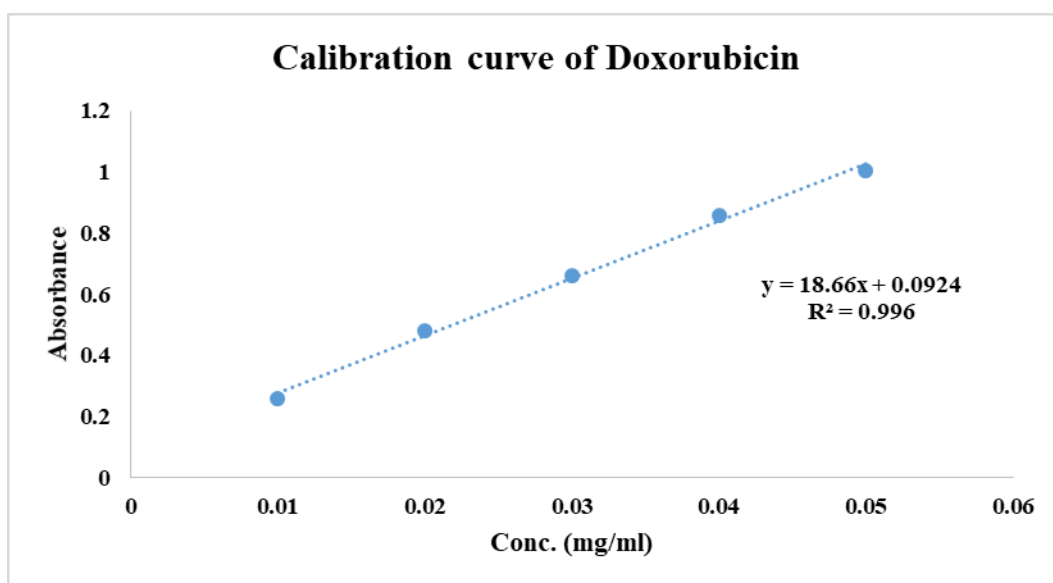


Figure 3.3: Calibration curve of Dox in distilled water at λ_{\max} 485nm.

3.2.3.2 Calibration curve of Mannose

The loaded amount of mannose was measured by spectrophotometry using anthrone method [57, 58]. A calibration curve of mannose has been done at λ_{\max} 620 nm and R^2 was 0.9966, figure 3.4. The loaded amount of mannose on SWCNTs was about 19 μ g/mg of *f*-SWCNTs (11).

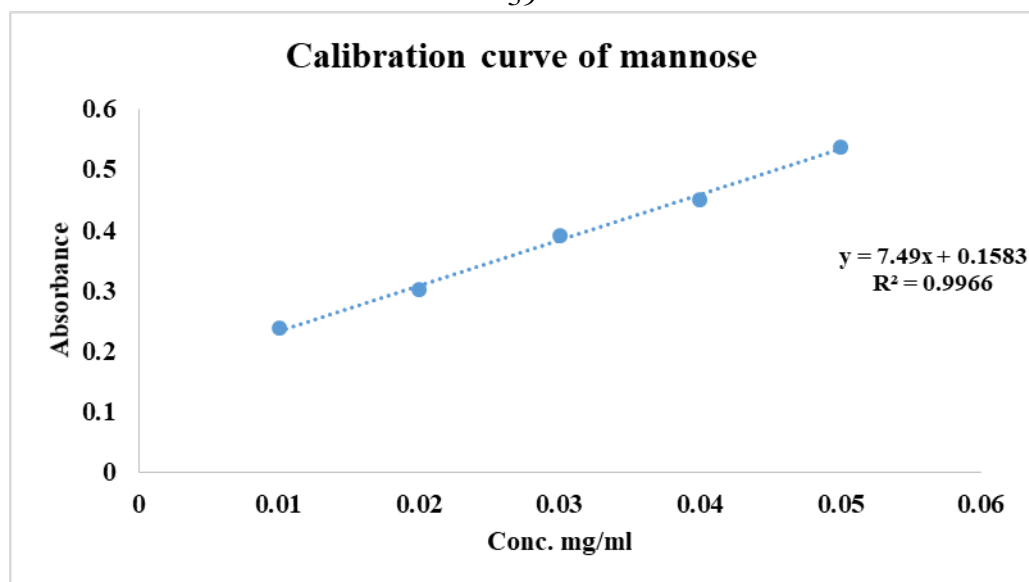


Figure 3.4: Calibration curve of Mannose in distilled water at λ_{\max} 620nm.

3.2.4 Thermogravimetric analysis (TGA)

A thermogravimetric analysis was conducted in order to quantify the total amount of the functionalization on the surface of the single walled carbon nanotubes in both final compounds (**7**) and (**11**). Both samples were heated at a constant rate until 600 °C as the SWCNTs are stable at this temperature and does not show any degradation as shown in figure 3.5. Therefore, the percentages of degradation are directly proportion to the total amounts of the percentage of functionalization. As shown in figure 3.5, a 25% of mass loss was observed that demonstrates the total percentage of the whole mono-functionalization of SWCNTs with the DOX attached with the hydrolysable linker. However, in the case of the dual functionalization of the SWCNTs in compounds (**11**) a higher amount was obtained with a 51% of functionalization, which corresponds to both

molecules the mannose as targeting agent and the doxorubicin attached to the linker.

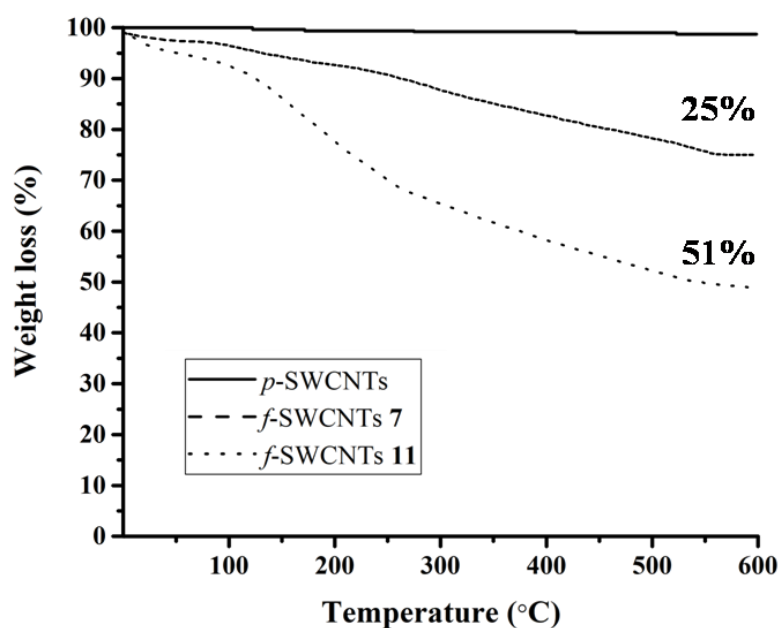


Figure 3.5: TGA results of *p*-SWCNTs, *f*-SWCNTs (7), *f*-SWCNTs (11).

3.3 *In vitro* drug release

It was mentioned in the introduction that the pH environment of cancer cells and tissue is acidic due to the production of lactic acid as the consequence of metabolic process in the cancer cells. Therefore, we took the advantage of this specific condition in the cancer; we have connected the doxorubicin with an acidic labile bond that can permit the release of the anticancer drug at acidic pH inside the cancer cells. Therefore, to study this behavior, we have investigated the release profiles of our drugs (7) and (11) at pH 7.4 and pH 5.5 with gentle agitation at 37°C. As shown in table 3.1 and figure 3.6, we can observe a time dependent cumulative release profiles

of Dox were achieved. In the case of *f*-SWCNTs (7), it was noticed that the release of DOX was only 45% at pH 7.4 while the release was about 98% after 5 h pH 5.5. However, the *f*-SWCNTs (11) showed the same behavior but the release at acidic pH was reached the 75% after 5h this could be due to the dual functionalization of the SWCNTs. We can conclude that Dox will be released in selective manner inside the cancer cells and its release will be minimum in the normal cells which could contribute to less side effects of the normal cells.

Table 3.1: Cumulative release data of Dox from *f*-SWCNT (7) and *f*-SWCNTs (11) at pH 7.4 and pH 5.5.

Time (hr) pH	<i>f</i> -SWCNTs (7)		<i>f</i> -SWCNTs (11)	
	5.5	7.4	5.5	7.4
0	0	0	0	0
0.25	30.25	25	28	32
0.30	34	30	32	35
0.75	40	32	35	40
1	44	33	40	40
1.25	48	36	45	45
1.30	55	38	52	47
1.75	62	40	57	48
2	66	40	59	50
2.5	70	40	64	51
3	75	42	67	52
3.5	81	44	68	52.5
4	85	46	73	53
4.5	90	46	75	53
17	98.306	46	77	53.5
17.5	98	46	78	54
18	98	46	78.5	54.5
18.5	98	46	78.5	54.5
19	98	46	78.5	54.5

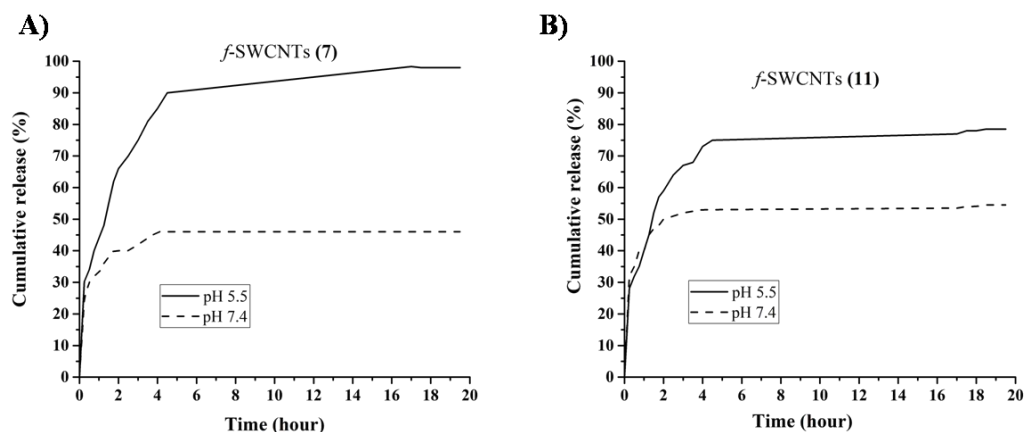


Figure 3.6: *In vitro* release of Dox from A) *f*-SWCNT (7); B) *f*-SWCNTs (11) at pH 7.4 and pH 5.5.

3.4 Anticancer activity

HepG2 and MCF-7 cell lines were used to investigate the therapeutic efficacy of Dox-SWCNTs and Dox-mannose-SWCNTs. Free Dox and blank CGM were used as controls. Since the release of Dox from SWCNTs is pH-dependent, the effect of different pH (normal 7.34, 7.0 and 6.5) on the quality of cells was initially evaluated by microscopic visualization of the cell morphology, which demonstrated that such pH values were well-tolerated by the cells. On the next step, the cells were incubated overnight with different concentrations of the test substances (0.5, 1.0, 2.0 and 4.0 mcg/ml) under the different pH. Here at normal pH, treatment with free Dox induced clear changes in cell morphology, as the majority of the cells became rounded and detached, this effect was very weak by compound (11) and compound (7) (appendix 1). Interestingly, along with the decrease in the pH of the medium the cytotoxicity of compounds 11 and 7 become

evident with highest effect at pH 6.5, which is close to the pH of cancer tissues [53].

In order to semi quantify the cytotoxic effect of the treatment the MTS *assay* was employed.

As depicted in figure 3.7 and figure 3.8 for HepG2 and MCF-7 cells under normal pH, Dox was able to induce cytotoxicity only at 4mcg/ml, where the percentage of viable cells was about 60% and 40%, respectively. Whereas Dox-SWCNTs could induce cytotoxicity at 1, 2 and 4 mcg/ml, where the cell viability was about 70, 65 and 40% respectively, which suggests that SWCNT could facilitate the entry of Dox. This effect was less than that of Dox-mannose-SWCNTs where the cytotoxicity was observed only at 2 and 4 mcg/ml, with cell viability of about 61 and 47% respectively (figure 3.7A) and for MCF-7 cell line was about 80% and 60% respectively, which suggests that the presence loading of mannose could slightly reduce the uptake of the complex, probably due to the increase in the molecular weight of the complex. Interestingly, when the pH of the medium was reduced to 7 and 6.5, a concentration-dependent cytotoxicity was observed by almost all of the used concentrations, (figure3.7B and 3.7C) and (figure3.8B and 3.8C). In order to evaluate precisely the pH effect on the activity of the test substances, statistical analysis was implemented for the concentration of 4 mcg/ml of each substance at different pH values. As shown in figure 3.7 and figure 3.8 although the reduction of the medium's pH could enhance the cytotoxicity of all test

substances, there was no significant difference between pH 7.0 and 6.5, implying that only a slight reduction in the physiological pH could be enough to obtain adequate cytotoxicity, which might be an advantage for targeting cancer tumor tissues.

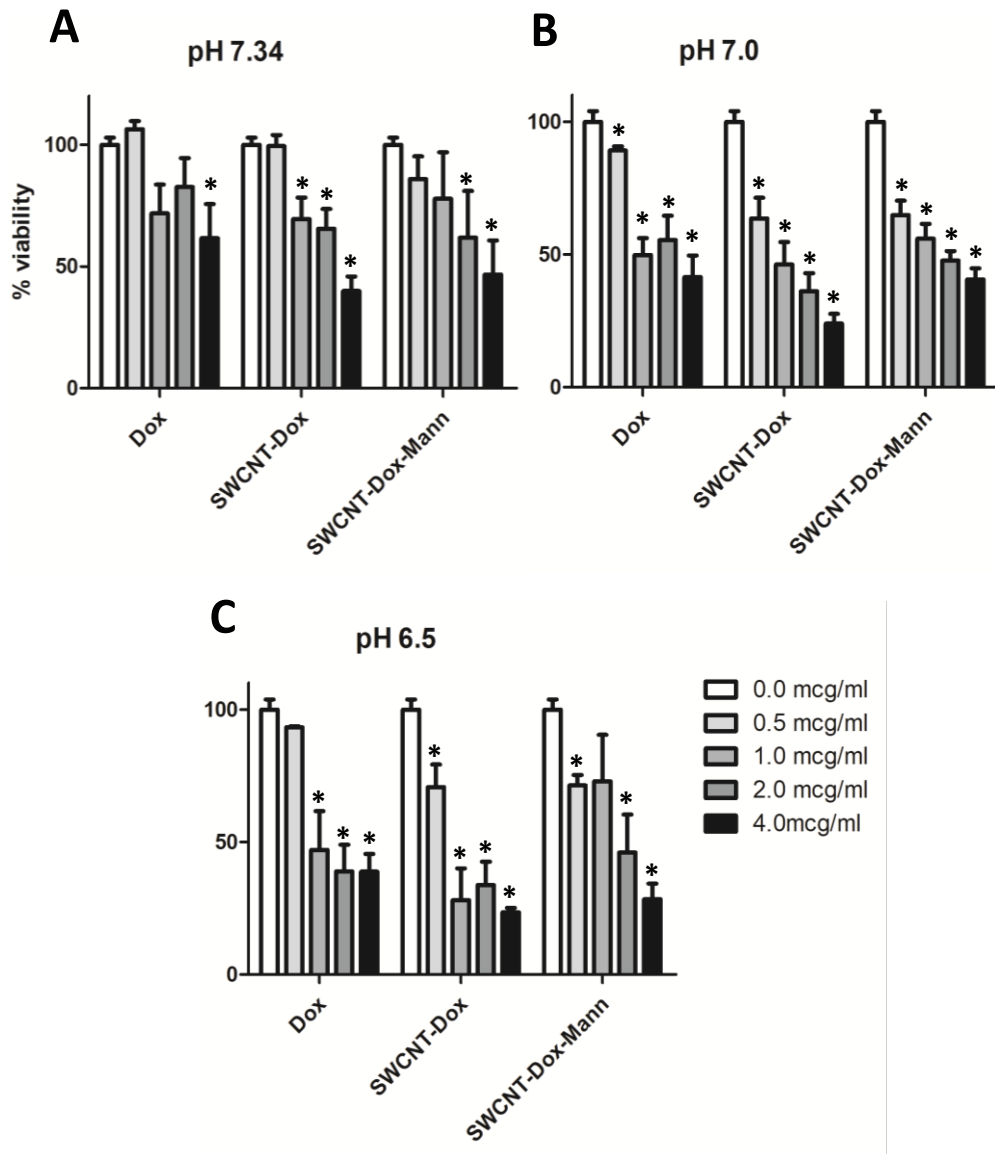


Figure 3.7: Concentration-dependent effect on cell viability (HepG2 cell) at different pH values. (n=6, *p<0.05, compared to 0.0 mcg/ml).

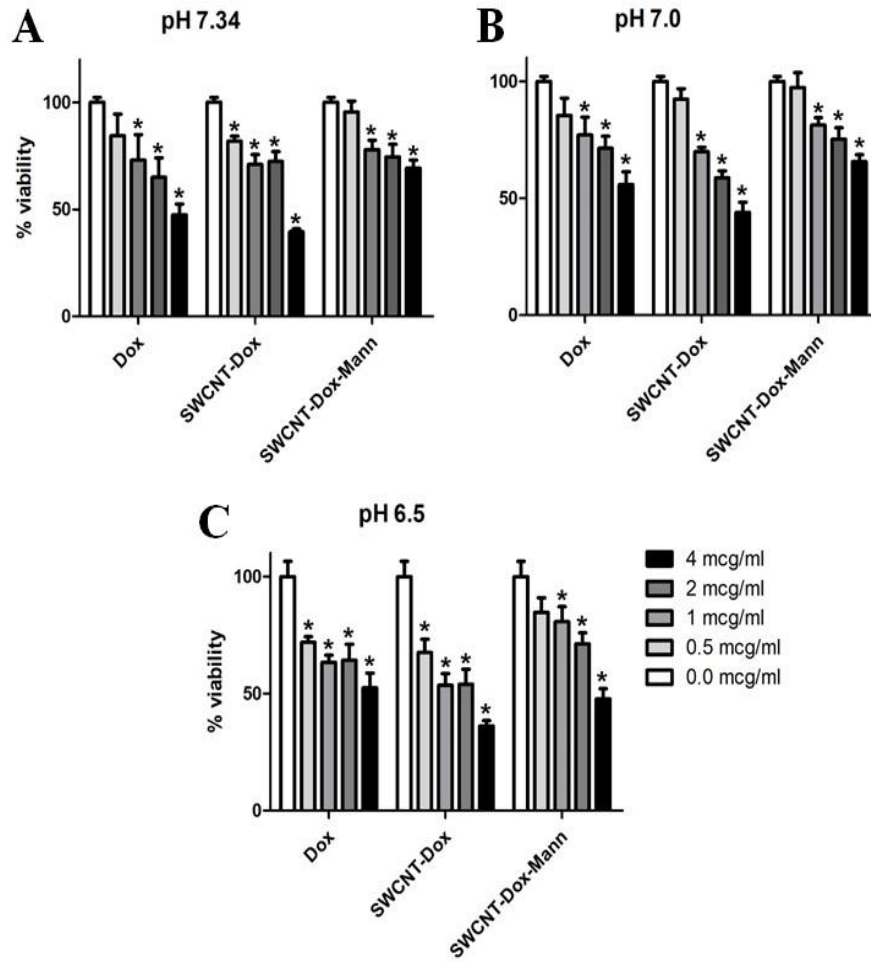


Figure 3.8: Concentration-dependent effect on cell viability (MCF-7 cell) at different pH values. (n=6, *p<0.05, compared to 0.0 mcg/ml).

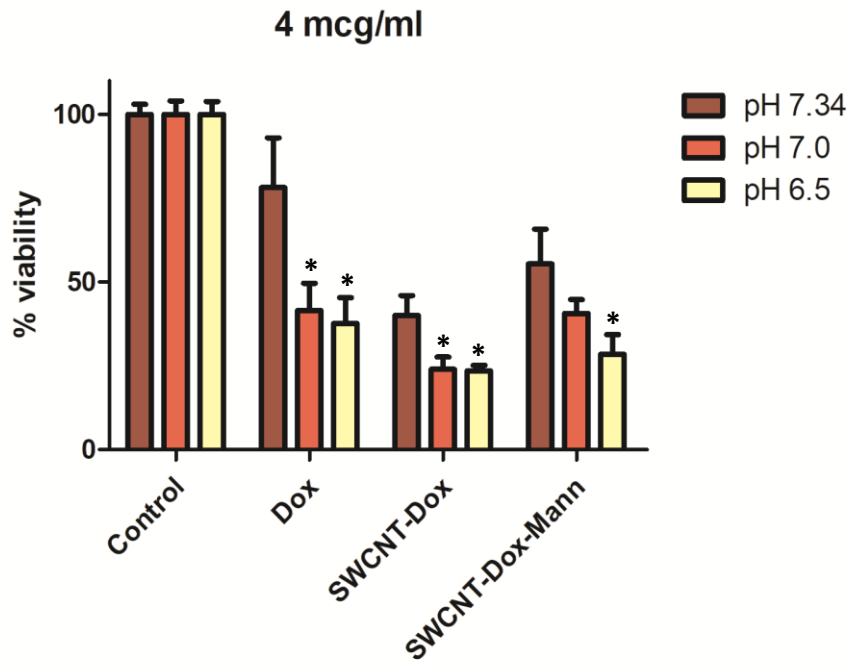


Figure 3.9: pH-dependent effect for 4 mcg/ml of each of the test substance on cell viability of HepG2 cells at different pH values. (n=6, *p<0.05, compared to control).

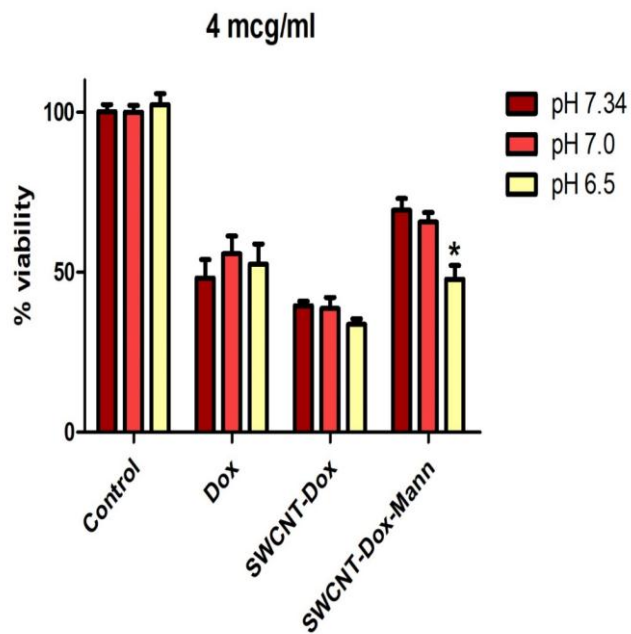


Figure 3.10: pH-dependent effect for 4 mcg/ml of each of the test substance on cell viability of MCF-7 cells at different pH values. (n=6, *p<0.05, compared to control).

As shown above in figure 3.9 and figure 3.10, the loading of mannose on SWCNT could slightly reduce the cytotoxicity of the complex. We hypothesized that mannose might facilitate receptor-mediated endocytosis. In order to test this hypothesis the cells were incubated with CGM supplemented by different concentrations of mannose for 30 min before the medium was exchanged for CGM with pH adjusted to 6.5 and supplemented with 4 mcg/ml of either of the test substances. After about 24 hr, MTS assay was performed. As shown in figure 3.11 and figure 3.12, the pre-incubation with any of the tested concentrations of mannose reduced the cytotoxicity of Dox-mannose-SWCNTs by approximately 40-57% in HepG2 and about 100% at MCF-7, suggesting that the entry of this complex might be dependent on mannose receptors, which imparts this complex a kind of selectivity for cancer cells that overexpress this type of receptors.

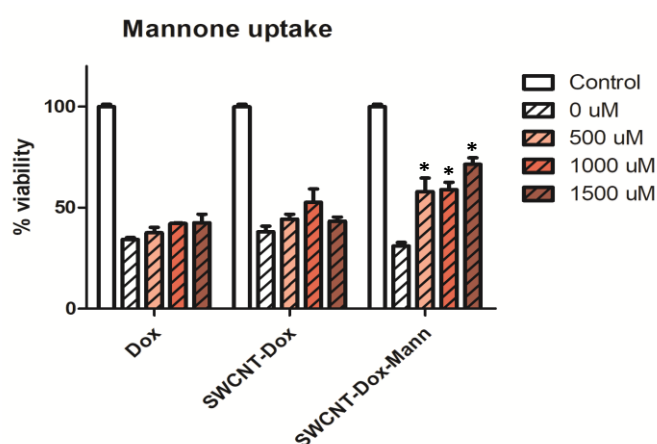


Figure 3.11: Effect of pre-incubation with mannose on the cytotoxicity of different test substances in HepG2 cell line at a concentration 4 mcg/ml and a pH of 6.5 (n=3, *p<0.05, compared to 0µM mannose).

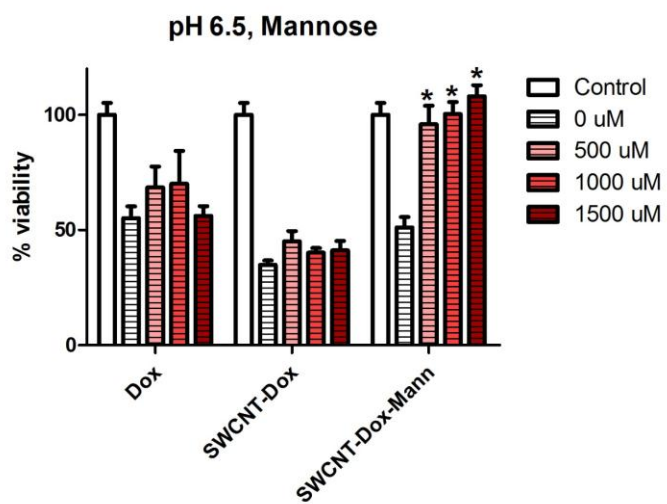


Figure 3.12: Effect of pre-incubation with mannose on the cytotoxicity of different test substances in MCF-7 cell line at a concentration 4 mcg/ml and a pH of 6.5 (n=3, *p<0.05, compared to 0 μ M mannose).

Conclusion

The covalent functionalization of SWCNTs with Dox has successfully been obtained. Moreover, dual functionalization has been achieved with the targeting agent, mmanose. The functionalization demonstrated good dispersibility of the *f*-SWCNTs as confirmed by TEM. The degree of functionalization was 25% and 51% for compound (7) and (11) respectively as confirmed by TGA. The *in vitro* release profile demonstrated that 45% of the loaded Dox was released within 18 hrs from the Dox-SWCNTs (7) at pH 7.4 and almost complete release at pH 5.5 at 37 °C. However, about 75% from the loaded drug was released within 5hr from Dox-Man-SWCNTs at pH 5.5 at 37 °C. Referring to the anticancer activity, the MTS proliferation assay showed that 4µg/ml of all compounds at pH 6.5 is the most adequate concentration to provide a good anticancer activity. Moreover, the mannose receptor selectivity test result showed that the compound (11) has mannose receptor selectivity that result to target the cancer cell which express mannose receptor.

References

1. **World Health Organization (WHO).** *Cancer*. 2017 [cited 2017 July, 30]; Available from: <http://www.who.int/cancer/en/>.
2. Jankowski, J.A., **Inflammation and gastrointestinal cancers**. Vol. 185. 2011: Springer Science & Business Media.
3. Wirtz, D., K. Konstantopoulos, and P.C. Searson, **The physics of cancer: the role of physical interactions and mechanical forces in metastasis**. *Nat Rev Cancer*, 2011. **11**(7): p. 512-22.
4. Nishida, N., et al., **Angiogenesis in cancer**. *Vasc Health Risk Manag*, 2006. **2**(3): p. 213-9.
5. Eberhard, A., et al., **Heterogeneity of angiogenesis and blood vessel maturation in human tumors: implications for antiangiogenic tumor therapies**. *Cancer research*, 2000. **60**(5): p. 1388-1393.
6. Folkman, J., **Angiogenesis in cancer, vascular, rheumatoid and other disease**. *Nature medicine*, 1995. **1**(1): p. 27-30.
7. Dvorak, H.F., et al., *Identification and characterization of the blood vessels of solid tumors that are leaky to circulating macromolecules*. *The American journal of pathology*, 1988. **133**(1): p. 95.
8. Iyer, A.K., et al., **Exploiting the enhanced permeability and retention effect for tumor targeting**. *Drug discovery today*, 2006. **11**(17): p.812-818.

9. Rocha, M., N. Chaves, and S. Bao, **Nanobiotechnology for Breast Cancer Treatment**. 2017.
10. Delaney, G., et al., **The role of radiotherapy in cancer treatment**. *Cancer*, 2005. **104**(6): p. 1129-1137.
11. Brahmer, J.R., et al., **Safety and activity of anti-PD-L1 antibody in patients with advanced cancer**. *N Engl J Med*, 2012. **2012** (366): p. 2455-2465.
12. Dougan, M. and G. Dranoff, **Immunotherapy of cancer, in Innate immune regulation and cancer immunotherapy**. 2012, Springer. p. 391-414.
13. Lindley, C., et al., **Perception of chemotherapy side effects cancer versus noncancer patients**. *Cancer practice*, 1999. **7**(2): p. 59-65.
14. Wang, B., et al., *Effect of different catalyst supports on the (n, m) selective growth of single-walled carbon nanotube from Co-Mo catalyst*. *Journal of materials science*, 2009. **44** (12): p. 3285-3295.
15. Upponi, J.R. and V.P. Torchilin, **Passive vs. Active Targeting: An Update of the EPR Role in Drug Delivery to Tumors, in Nano-Oncologicals**. 2014, Springer. p. 3-45.
16. Sutradhar, K.B. and M.L. Amin, **Nanotechnology in cancer drug delivery and selective targeting**. *ISRN Nanotechnology*, 2014. **2014**.

17. Calvaresi, E.C. and P.J. Hergenrother, **Glucose conjugation for the specific targeting and treatment of cancer**. *Chemical science*, 2013. **4**(6): p. 2319-2333.
18. Li, L., et al., **Mannose-conjugated layered double hydroxide nanocomposite for targeted siRNA delivery to enhance cancer therapy**. *Nanomedicine: Nanotechnology, Biology and Medicine*, 2017.
19. He, Q.L., et al., **Targeted delivery and sustained antitumor activity of triptolide through glucose conjugation**. *Angewandte Chemie*, 2016. **128** (39): p. 12214-12218.
20. Ahire, J.H., et al., **Synthesis of D-mannose capped silicon nanoparticles and their interactions with MCF-7 human breast cancerous cells**. *ACS applied materials & interfaces*, 2013. **5**(15): p.7384-7391.
21. Yin, L., et al., **Biodegradable Micelles Capable of Mannose-Mediated Targeted Drug Delivery to Cancer Cells**. *Macromolecular rapid communications*, 2015. **36** (5): p. 483-489.
22. Guo, X., et al., **pH-triggered intracellular release from actively targeting polymer micelles**. *Biomaterials*, 2013. **34** (18): p. 4544-4554.
23. Stubbs, M., et al., **Causes and consequences of tumour acidity and implications for treatment**. *Molecular medicine today*, 2000. **6**(1): p. 15-19.

24. Iannazzo, D., et al., **Recent advances in carbon nanotubes as delivery systems for anticancer drugs.** *Current medicinal chemistry*, 2013. **20** (11): p. 1333-1354.
25. Cheng, L.-C., et al., **Nano–bio effects: interaction of nanomaterials with cells.** *Nanoscale*, 2013. **5**(9): p. 3547-3569.
26. Kashiwagi, T., et al., **Relation between the viscoelastic and flammability properties of polymer nanocomposites.** *Polymer*, 2008. **49**(20): p. 4358-4368.
27. Li, Z., Z. Wu, and K. Li, **The high dispersion of DNA–multiwalled carbon nanotubes and their properties.** *Analytical biochemistry*, 2009. **387**(2): p. 267-270.
28. Collins, P.G., M.S. Arnold, and P. Avouris, **Engineering carbon nanotubes and nanotube circuits using electrical breakdown.** *science*, 2001. **292**(5517): p. 706-709.
29. Zhao, Y., G. Xing, and Z. Chai, **Nanotoxicology: are carbon nanotubes safe?** *Nature nanotechnology*, 2008. **3**(4): p. 191-192.
30. Wu, H.-C., et al., *Chemistry of carbon nanotubes in biomedical applications.* *J. Mater. Chem.*, 2010. **20**(6): p. 1036-1052.
31. Liu, Z., et al., **Carbon materials for drug delivery & cancer therapy.** *Materials today*, 2011. **14**(7): p. 316-323.

32. Fujigaya, T. and N. Nakashima, **Non-covalent polymer wrapping of carbon nanotubes and the role of wrapped polymers as functional dispersants**. *Science and technology of advanced materials*, 2015. **16**(2): p. 024802.
33. Debnath, S., et al., *A study of the interaction between single-walled carbon nanotubes and polycyclic aromatic hydrocarbons: toward structure–property relationships*. *The Journal of Physical Chemistry C*, 2008. **112**(28): p. 10418-10422.
34. Angelikopoulos, P., et al., *Dispersing individual single-wall carbon nanotubes in aqueous surfactant solutions below the cmc*. *The Journal of Physical Chemistry C*, 2009. **114**(1): p. 2-9.
35. Gao, J., et al., *Selective wrapping and supramolecular structures of polyfluorene–carbon nanotube hybrids*. *ACS nano*, 2011. **5**(5): p. 3993-3999.
36. Zhao, Y.-L. and J.F. Stoddart, **Noncovalent functionalization of single-walled carbon nanotubes**. *Accounts of chemical research*, 2009. **42**(8): p. 1161-1171.
37. Prencipe, G., et al., *PEG branched polymer for functionalization of nanomaterials with ultralong blood circulation*. *Journal of the American Chemical Society*, 2009. **131**(13): p. 4783-4787.

38. Guldi, D.M., et al., *Supramolecular Hybrids of [60] Fullerene and Single-Wall Carbon Nanotubes*. *Chemistry-A European Journal*, 2006. **12**(15): p. 3975-3983.
39. Yang, K., L. Zhu, and B. Xing, **Adsorption of polycyclic aromatic hydrocarbons by carbon nanomaterials**. *Environmental science & technology*, 2006. **40**(6): p. 1855-1861.
40. Assali, M., et al., **Non-covalent functionalization of carbon nanotubes with glycolipids: glyconanomaterials with specific lectin-affinity**. *Soft Matter*, 2009. **5**(5): p. 948-950.
41. Kushwaha, S.K.S., et al., *Carbon nanotubes as a novel drug delivery system for anticancer therapy: a review*. *Brazilian Journal of Pharmaceutical Sciences*, 2013. **49**(4): p. 629-643.
42. Bahr, J.L., et al., *Functionalization of carbon nanotubes by electrochemical reduction of aryl diazonium salts: a bucky paper electrode*. *Journal of the American Chemical Society*, 2001. **123**(27): p. 6536-6542.
43. Tagmatarchis, N. and M. Prato, *Functionalization of carbon nanotubes via 1, 3-dipolar cycloadditions*. *Journal of materials chemistry*, 2004. **14**(4): p. 437-439.
44. Zamolo, V.A., E. Vazquez, and M. Prato, **Carbon Nanotubes: Synthesis, Structure, Functionalization, and Characterization**, in *Polyarenes II*. 2013, Springer. p. 65-109.

45. Rao, C.N.R., et al., **Nanotubes**. *ChemPhysChem*, 2001. **2**(2): p.78-105.
46. Dyke, C.A. and J.M. Tour, *Solvent-free functionalization of carbon nanotubes*. *Journal of the American Chemical Society*, 2003. **125**(5): p. 1156-1157.
47. **DRUG BANK**. *Doxorubicin*. [cited 2017 Dec, 9]; Available from: <https://www.drugbank.ca/drugs/DB00997>.
48. British pharmacopia. *Doxorubicin Hydrochloride* 2017.
49. Vos, K.J., et al., *A multi-compartment pharmacokinetic model of the interaction between paclitaxel and doxorubicin*. *EPJ Nonlinear Biomedical Physics*, 2014. **2**(1): p. 13.
50. **National Cancer Insitute**. *Doxorubicin*. [cited 2017 Dec, 9]; Available from: <https://www.cancer.gov/search/results>.
51. Mobaraki, M., et al., *Molecular Mechanisms of Cardiotoxicity: A Review on Major Side-effect of Doxorubicin*. *Indian Journal of Pharmaceutical Sciences*, 2017. **79**(3).
52. Kratz, F., *Acid-sensitive prodrugs of doxorubicin, in Anthracycline chemistry and biology II*. 2007, Springer. p. 73-97.
53. Bae, Y., et al., *Multifunctional polymeric micelles with folate-mediated cancer cell targeting and pH-triggered drug releasing*

properties for active intracellular drug delivery. *Molecular BioSystems*, 2005. **1**(3): p. 242-250.

54. You, J., G. Zhang, and C. Li, **Exceptionally high payload of doxorubicin in hollow gold nanospheres for near-infrared light-triggered drug release.** *ACS nano*, 2010. **4**(2): p. 1033-1041.

55. Mo, Y., et al., **Controlled release and targeted delivery to cancer cells of doxorubicin from polysaccharide-functionalised single-walled carbon nanotubes.** *Journal of Materials Chemistry B*, 2015. **3**(9): p. 1846-1855.

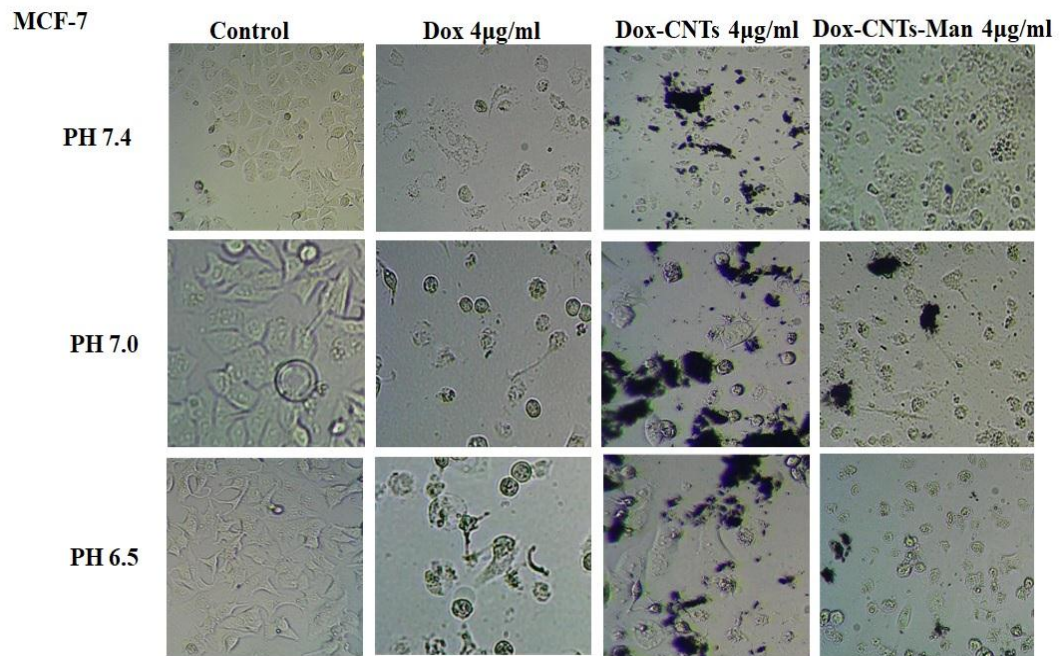
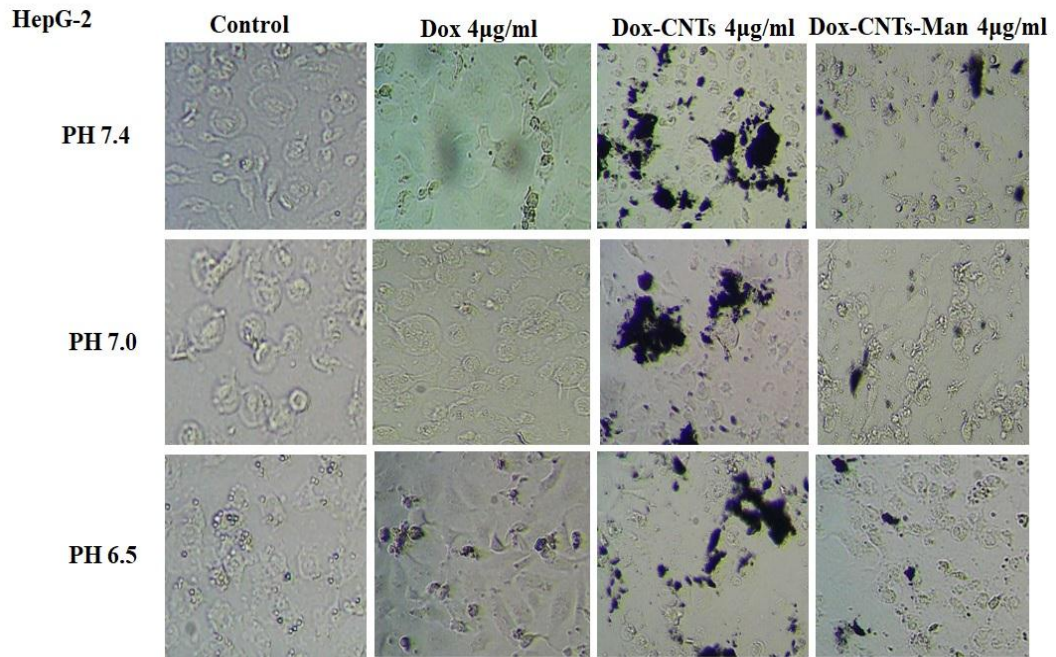
56. Gu, Y.-J., et al., *Development and evaluation of pH-responsive single-walled carbon nanotube-doxorubicin complexes in cancer cells.* *International journal of nanomedicine*, 2011. **6**: p. 2889.

57. Ashwell, G., [12] **Colorimetric analysis of sugars.** 1957.

58. Scott Jr, T.A. and E.H. Melvin, **Determination of dextran with anthrone.** *Analytical Chemistry*, 1953. **25**(11): p. 1656-1661.

59. EUROPEAN PHARMACOPOEIA 7.0. **BUFFER SOLUTIONS.**, 2011, ; Available from:

<http://www.drugfuture.com/Pharmacopoeia/EP7/DATA/40103E.PDF>.

Appendix I

جامعة النجاح الوطنية

كلية الدراسات العليا

التفعيل الإزدواجي لأنابيب الكربون النانوية أحادية الجدران في علاج السرطان المستهدف

إعداد

صفاء رائد عبد الحافظ دية

إشراف

د. محي الدين العسالي

د. نعيم كتانة

قدمت هذه الأطروحة استكمالاً لمتطلبات الحصول على درجة الماجستير في العلوم الصيدلانية،
بكلية الدراسات العليا، في جامعة النجاح الوطنية، نابلس - فلسطين.

2018

ب

التفعيل الإزدواجي لأنابيب الكربون النانوية أحادية الجدران في علاج السرطان المستهدف

إعداد

صفاء رائد عبد الحافظ دية

إشراف

د. محي الدين العسالي

د. نعيم كتانة

الملخص

العلاج الكيميائي هو استراتيجية أساسية في علاج السرطان. لكنه يسبب اثار جانبية خطيرة بسبب تأثيره على الخلايا الطبيعية إلى جانب الخلايا السرطانية. لذلك، طور العديد من الباحثين أنظمة جديدة لتوصيل الدواء قد تساعد على تقليل الآثار الجانبية والجرعة الفعالة للدواء بالإضافة إلى استهداف الخلايا السرطانية فقط بالعلاج الكيميائي. تعتمد إحدى أنظمة توصيل الدواء في هذا المجال على تكنولوجيا أنابيب الكربون النانوية.

الهدف من هذا البحث هو ربط دواء الدكسوروبيسين مع انابيب الكربون النانوية أحادية الجدران من خلال رابطة تساهمية باستخدام مشتق ايثيلين غلايكول لتحسين للدواء مع هذا النظام. إضافة إلى ذلك، تم تزويد هذا النظام بعامل استهداف وهو سكر المنوز ليستهدف الخلايا السرطانية عوضا عن الخلايا الطبيعية.

ولقد أظهر تحليل الدواء النانوي بواسطة المجهر الالكتروني النافذ تفرق وتوزع جيد للأنابيب النانوية بقطريتراوح بين (6-10) نانومتر. بالإضافة الى ذلك، تم تحديد كفاءة التفعيل لأنابيب الكربون النانوية بواسطة جهاز التحليل الحراري الذي أظهر بنسبة 25% لأنابيب الكربونية المحملة بالدكسوروبيسين وبنسبة 51% لأنابيب الكربونية المحملة بالدكسوروبيسين منوز

وأظهرت دراسة نمط خروج الدواء من انابيب الكربون النانوية أن حوالي 45% من الدواء قد خرج من انابيب الكربون المحملة بالدكسوروبيسين(7) على درجة حموضة 7.4 عند 37 درجة مئوية وإطلاق شبه كامل من نفس المركب على درجة حموضة 5.5 عند نفس درجة الحرارة. بينما أن

نسبة خروج الدواء من أنابيب الكربون النانوية المحملة بالدوكسوروبيسين منوز (11) على مدار 5 ساعات كانت 75% على درجة حموضة 5.5 عند 37 درجة مئوية.

أما فيما يخص دراسة تأثير السمية والنشاط المضاد للسرطان، تمت الدراسة للمركبات المذكورة أعلاه، بتراكيز وظروف مختلفة. وقد لوحظ التركيز الأعلى سمية هو 4 ميكروغرام/مل عند درجة حموضة 6.5. أما بالنسبة لدراسة الانتقائية لمستقبل المنوز، فقد قلت نسبة السمية بحوالي 40-57% بعد الاحتضان المسبق للمنوز بتراكيز مختلفة، مما يشير أن دخول هذا المركب يعتمد على نسبة مستقبلات المنوز الفعالة، مما يضيف نوعاً من الانتقائية للخلايا السرطانية مقارنة بالخلايا الطبيعية.

